ACS Chemical Neuroscience pubs.acs.org/acschemicalneuroscience Review

Superparamagnetic Iron Oxide Nanoparticles: Promises for Diagnosis and Treatment of Multiple Sclerosis

Morteza Mahmoudi,*,† Mohammad A. Sahraian,‡,§ Mohammad A. Shokrgozar,† and Sophie Laurent∥

†National Cell Bank, Pasteur Institute of Iran, Tehran, 11365-8639, Iran, ‡Department of Neurology, and §Sina MS Research Center, Sina Hospital, Tehran University of Medical Sciences, Tehran, Iran, and ∥Department of General, Organic, and Biomedical Chemistry, NMR and Molecular Imaging Laboratory, University of Mons, Avenue Maistriau, 19, B-7000 Mons, Belgium

Abstract

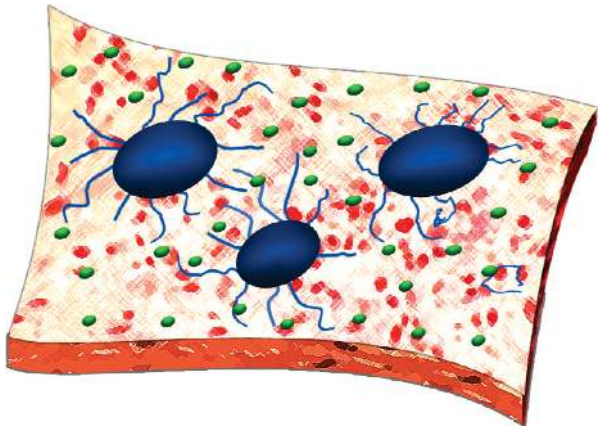

Smart superparamagnetic iron oxide nanoparticles (SPIONs) are the most promising candidate for theragnosis (i.e., diagnosis and treatment) of multiple sclerosis. A deep understanding of the dynamics of the in vivo neuropathology of multiple sclerosis can be achieved by improving the efficiency of various medical techniques (e.g., positron emission tomography and magnetic resonance imaging) using multimodal SPIONs. In this Review, recent advances and challenges in the development of smart SPIONs for theragnostic applications are comprehensively described. In addition, critical outlines of emerging developments are provided from the points of view of both clinicians and nanotechnologists.

Keywords: Superparamagnetic iron oxide nanoparticles, theragnosis, multiple sclerosis, neuropathology, multimodality

Multiple sclerosis (MS) is a chronic demyelinating disease of the central nervous system (CNS) that usually affects young adults. The disease is diagnosed throughout the world with more than two million affected individuals. Although the disease was recognized in the 19th century, there were limited data on the diagnosis, pathophysiology, and management of MS until the last 50 years. With every step of progress in immunology, imaging, and biotechnology, there was indeed progress in our understanding of the etiology, diagnosis, and treatment of this disease. Before the era of magnetic resonance imaging (MRI) began, diagnosis of MS was mainly dependent on the medical history and clinical examination of the patient. With the application of MRI by Young et al. in 1983, a revolutionary step took place in this field (*1*, *2*). MRI played an expanding and unique role in the diagnosis of the disease. Nowadays, conventional MRI is used for early diagnosis, predicting the prognosis, and evaluating the response to the therapeutic agents considered for clinical trials. In fact, the diagnostic criteria changed twice during the past decade as MRI showed its power for early depiction of the disease and reliably excluding other differential diagnosis (*3*, *4*). With more advances in MRI techniques and the introduction of nonconventional MRI, such as MR spectroscopy, diffusion tensor, magnetization transfer, and functional MRI, into the field, our knowledge about the pathology and evolution of the disease was extensively improved. These techniques enabled investigators to measure the actual extent of tissue damage related to MS and to better characterize the nature and the functional consequences of such damages (*5*, *6*). They also emphasized the previously ignored neurodegenerative aspect of the disease and opened a new window on the interaction between neuroinflammation and neurodegeneration to induce permanent disability (*7*). With advances in laboratory medicine and biotechnology, different preparations of interferon beta were developed to control the exacerbations in MS and rapidly became commercially available for patients. These drugs are partially effective and cannot cure the disease. With the recognition of different types of receptors on leukocytes and their major role in induction of inflammation, a new class of drugs called monoclonal antibodies was applied to decrease disability and exacerbation in MS by inhibiting the activity of lymphocytes or their migration into the CNS. This new class of drugs resulted in a better disease control despite the serious but rare side effects (*8*).

The era of nanotechnology began about 50 years ago when Richard Feynman in his seminal lecture said

Received Date: November 3, 2010
Revised Manuscript Received: December 8, 2010
Published on Web Date: February 04, 2011

DOI: 10.1021/cn100100e | *ACS Chem. Neurosci.* (2011), *2*, 118–140

"there is plenty of room at the bottom". From then on, extensive efforts have been devoted to congregate nanotechnology and medicine, leading to the new interdisciplinary field of nanomedicine. This new field has brought together engineers, physicists, biologists, chemists, mathematicians, and physicians to improve detection, imaging, and drug delivery devices. To accelerate the war on cancer, declared in 1971 by U.S. President Richard Nixon, the National Cancer Institute launched the Alliance for Nanotechnology in Cancer in 2004. Since then, significant funds have been devoted to the development and improvement of nanotechnologies in order to reduce cancer mortality (*9*).

Theragnostics is a strategy that integrates therapeutics with diagnostics to develop new personalized treatments with enhanced efficacy and safety. In this approach, which is the final goal of nanomedicine, scientists are looking for multifunctional nanomaterials which are able for coincident disease diagnosis, drug delivery, monitoring the drug delivery, and evaluation of treatment efficiency in a single nanoparticle platform (*10*).

In this Review, we will provide a brief overview on the history of MS and nanoscience, followed by some recent developments in superparamagnetic iron oxide nanoparticles (SPIONs) and their application in depicting MS lesions in the brain and spinal cord. Moreover, the ability to apply nanotechnology to some, if not all, aspects of MS research and clinical studies in the future will be discussed.

Multiple Sclerosis: A Historical Overview

The earliest recorded description of MS dates back to the 14th century, but it was the French neurologist Jean-Martin Charcot (1825−1893) who made the first definite links between the symptoms of MS and the pathological changes seen in post-mortem samples. He described the condition as "sclerose en plaques" and recognized MS as a distinct disease entity (*11*). In 1916, Dr. James Dawson described the inflammation around blood vessels and damage to the myelin. For many years, scientists thought that MS was caused by some forms of toxins and poisons. Since most MS damages were observed in the vicinity of blood vessels, it seemed reasonable that a circulating toxin, leaking into the brain tissue, could cause the damage. The viral etiology of MS was suspected when physicians faced a disease resembling MS after vaccination (especially against rabies). It was assumed that this occurred because the virus in the vaccines was not completely inactivated, and so it attacked the myelin. In 1935, Dr. Thomas Rivers successfully produced an MS-like illness in laboratory animals, under a virus free condition. This animal model of MS, called experimental allergic encephalomyelitis (EAE), paved the way to the theory of "autoimmunity" for this disease and soon became an important model for studying the immunology and treatments (*12*). In 1947, with a grant from the National MS Society, Dr. Elvin Kobat at Columbia University identified abnormal immunological proteins which appeared in a pattern known as oligoclonal bands in the spinal fluids of patients (*13*). In 1965, the National MS Society founded a panel of experts, headed by George Schumacher, to draw up standard guidelines for MS diagnosis. At the same time, a rating scale for disability measurement was proposed by Dr. John Kurtzke (*14*). These two steps allowed researchers to test possible MS treatments. In the 1960s, adrenocorticotrophic hormone (ACTH) was used to treat MS exacerbations. This was the first controlled trial of a successful treatment for MS. ACTH was soon replaced by high dose steroids which are currently used as the standard treatment for MS relapse. Steroids are, however, not effective at reducing the number of relapses or the rate of disease progression (*15*). This was followed in the 1970s and 1980s by trials with a variety of immunosuppressant agents, including cyclophosphamide, cyclosporine, azathioprine, methotrexate, and glatiramer acetate (GA) (copolymer 1) (*11*, *16*). In the late 1980s, the concept of immunomodulation was extensively explored, and this was assisted by the development of noninvasive monitoring methods. In 1981, Ian Young applied a new imaging technique, MRI, to visualize brain and spinal cord lesions in MS. He properly predicted the future value of MR imaging in diagnosis and monitoring of MS (*2*). A new era in the treatment of MS began in 1993 when the pivotal trial of Interferon beta 1b (Betaseron, IFNβ-1b) showed its potential to reduce the exacerbations of the disease. It was the first therapy which was proven effective in altering the natural history of relapsing-remitting MS (RRMS) (*17*, *18*). The IFNβ-1b study was followed in subsequent years by the introduction to the market of Interferon beta 1a (Avonex) (1996), the noninterferon agent GA (1996), and subcutaneous INF beta 1a (Rebif) (1998) as agents to decrease relapses in RRMS (*19*−*21*). In 1999, mitoxantrone (Novantron, a cytotoxic agent) was approved to change the course of progressive relapsing forms of MS (*22*). With a better understanding of the pathogenesis of the disease, there was a continued progress to improve therapeutic approaches for MS. The first monoclonal antibody, called natalizumab (Tysabri), was approved in 2006 (*23*). This drug could significantly suppress exacerbations in MS in several trials. Despite its rare but fatal side effect, called progressive multifocal encephalopathy, this drug is used in active patients. Fingolimod (Gilinya) was the first oral medication approved in 2010 for RRMS (*24*). It opened a new era in MS treatment, as many patients suffered from pain and injection site reactions due to interferons. A number

DOI: 10.1021/cn100100e | *ACS Chem. Neurosci.* (2011), *2*, 118–140

Table 1. Significant Progress in Nanoscience

year	reporter	remark	ref
1867	James Clerk Maxwell	It was proposed that a tiny entity entitled "Maxwell's Demon" is able to handle individual molecules.	*27*
1914	Richard Adolf Zsigmondy	By employing the dark field method via ultramicroscope, the detailed study of gold sols and other nanomaterials with sizes down to 10 nm and less were introduced; the first classification system based on nanoparticle size was developed.	(*28*, *29*)
1920s	Irving Langmuir and Katharine B. Blodgett	Development of monolayer formations.	*29*
1959	Richard Feynman	The real era of nanoscience and nanotechnology was proposed by his well-known sentence "There's plenty of room at the bottom."	*30*
1960	William H. McLellan	The first nanomotor was developed.	*31*
1974	Norio Taniguchi	The first time that the term "nanotechnology" is used in a scientific publication.	(*30*, *32*, *33*)
1974	Tuomo Suntola	Development of the process of depositing uniform one atomic layer thin films	*29*
1985	Tom Newman	Confirming the possibility of scaling down letters small enough so as to be able to fit the entire Encyclopedia Britannica on the head of a pin.	*34*

of oral medications, some disease-modifying and some for the improvement of symptoms, are currently in phase III trials that may lead to U.S. Food and Drug Administration approval in the near future.

Nanoscience, Nanotechnology, and Nanomaterials: A Historical Overview

Nanoscience and nanotechnology deal with matter on an atomic/molecular scale. More specifically, nanoscience and technology refer to the research and manufacturing development at ultrasmall scales (e.g., atomic), which leads to the desired manipulation of structures in the range of 1−100 nm, in at least one dimension.

From the public's point of view, nanotechnology is a relatively new development; however, it has been proven that the central conceptual developments in nanoscience, more specifically for nanoparticles, have been in use since 5000 years ago, when Egyptians ingested Au nanoparticles for mental and body purification (*25*). In addition to Egyptians, Persians also employed both Au and Ag nanoparticles in the 10th century BC for the fabrication of ceramic glazes to provide a lustrous or iridescent effect (*26*). The era of nanoscience began with the lecture of Nobel award winner, Richard Feynman, in 1959. Ever since, and thanks to the development of highly sophisticated characterization methods at the nanoscale, both the research and the technological aspects of nanoscience have grown explosively, particularly during the last two decades. Table 1 shows the significant improvements in the field of nanoscience and nanotechnology in the last 150 years. Figure 1 shows the classification of variousnanoparticles together with their most prominent

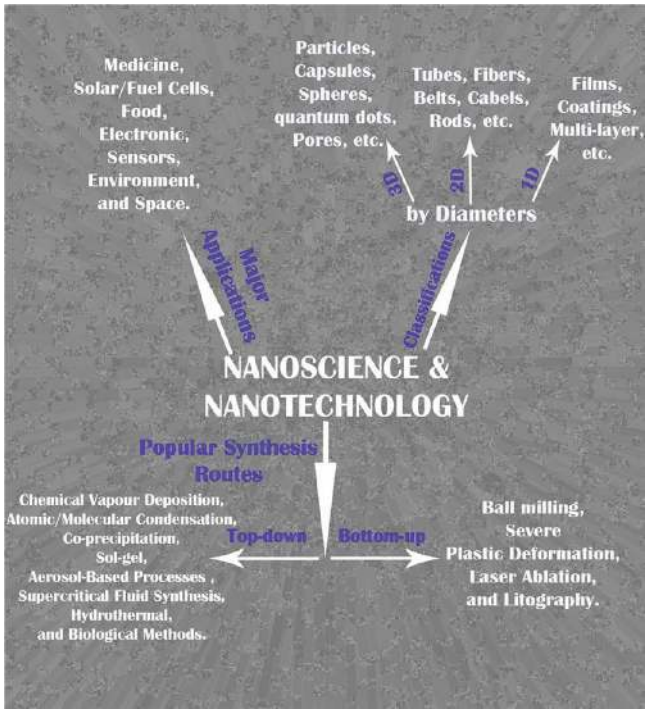

Figure 1. Most prominent classification, synthesis routes, and application of nanomaterials.

synthesis methods as well as their well-known applications. In addition, Table 2 also lists an overall classification of nanoparticles along with examples for each group.

Nanoparticles for Medical Applications

Nanomedicine has been recognized as a new emerging field of nanotechnology that introduced a new interface between nanotechnology and biotechnology,

DOI: 10.1021/cn100100e | *ACS Chem. Neurosci.* (2011), *2*, 118–140

Table 2. General Classification of Various Nanoparticles

main classes	examples	ref
metals	gold (Au), silver (Ag), platinum (Pt), and palladium (Pd)	(*35*−*37*)
metal oxides	silicon dioxide (SiO_2), titanium dioxide (TiO_2), aluminum dioxide (Al_2O_3), zinc oxide (ZnO), and iron oxide (Fe_2O_3, Fe_3O_4)	(*38*−*43*)
semiconductors	cadmium telluride (CdTe), cadmium selenide (CdSe), cadmium sulfate (CdS), titanium dioxide (TiO_2), and gallium arsenide (GaAs)	(*35*, *44*−*47*)
carbon black	carbon nanotubes and fullerenes	(*48*−*54*)
magnetic materials	iron oxide (Fe_3O_4, Fe_2O_3, and γ-Fe_2O_3), iron-palladium and cobalt, ferrimagnetic spinels, cobalt ferrite, $CoFe_2O_4$, Mn−Zn and Mn−Zn−Gd ferrite particles, copper nickel, ferromagnetic perovskites $La_{1-x}Sr_xMnO_3$, $Ni_{(1-x)}Cr_x$, gadolinium-, calcium-, and lanthanum complexes, and ferrimagnetic $SrFe_{12}O_{19}/\gamma$-Fe_2O_3 composites	(*55*−*73*)
polymers	polylactides (PLA), polyglycolides (PGA), poly(lactide-*co*-glycolides) (PLGA), polyanhydrides, polyorthoesters, and polycaprolactone	(*74*−*78*)
multi-classes	core−shell, magnetic beads, and colloidal nanocrystal clusters	(*79*−*83*)

the so-called "nano−bio interface" (*84*). Due to their novel physicochemical properties, nanomaterials offer great hopes for the creation of new theragnostic possibilities in medicine. Surface engineered nanomaterials have been comprehensively examined in a wide range of biomedical applications, including biomolecular imaging (*85*), novel drug delivery systems (*86*), targeting delivery/imaging (*81*), transfection (*87*), gene delivery (*88*), tissue engineering (*89*), and stem cell/cell/biomolecules tracking (*42*). Hence, nanomedicine products will grow at a rate of up to 17% annually of the percentage of product, to reach an estimated $53 billion market in 2011. The greatest share of the nanotechnology in pharmaceutical applications is expected to reach $18 billion in 2014 (*90*, *91*). However, the major shortcoming of using nanoparticles in biomedical applications is their possible cytotoxicity (*91*, *92*). In order to be used for safe and high yield biomedical applications, nanomaterials must be coated by ideal organic/inorganic materials which can satisfy the following requirements: (i) preventing the opsonization of nanomaterials; (ii) avoiding agglomeration of nanoparticles in biological medium; (iii) achieving the desired surface charge for the nanomaterials' main task; (iv) preserving the functionalities of the nanomaterials; (v) exhibiting the protein absorption on the surface of nanoparticles and their corresponding denaturation; and (vi) ensuring the biocompatibility of nanoparticles (*42*, *80*, *81*, *93*, *94*).

During the past decade, nanoparticles with multitask capability have attracted the attention of the scientific community (*69*). Multitask nanoparticles can satisfy several applications (e.g., drug delivery, thermotherapy, and imaging) simultaneously; hence, reducing both the patient resistance and the side effects of nanoparticles/drugs (*85*). In addition, multitask nanoparticles have increased the hopes for the early diagnostic and the fast treatment of catastrophic diseases (e.g., cancer) via their theragnostic capability (*85*). One of the outstanding candidates for theragnostic applications are magnetic nanoparticles. The main tasks of magnetic nanoparticles, for theragnostic applications, include visualization of the desired biospecies, guiding into preferred sites using a magnetic field, and heating in order to trigger drug release or to produce hyperthermia of desired tissues (*95*).

Superparamagnetic Iron Oxide Nanoparticles (SPIONs)

SPIONs are based on magnetite (Fe_3O_4) or maghemite (γ-Fe_2O_3) cores stabilized with a hydrophilic surface coating (polysaccharide, synthetic polymers, or small molecules) (*56*, *80*, *81*, *96*). Magnetic nanoparticles based on iron oxides or iron oxide shells are recognized as the most prominent magnetic materials, due not only to their great biocompatibility but also to their unique physicochemical properties (e.g., strong effects on T_1, T_2, and T_2* relaxation, inducing signal increase on T_1-weighted images and signal reduction on T_2-weighted-gradient-echo images) (*42*, *43*, *69*, *80*, *81*, *85*, *86*, *93*, *97*−*105*). SPIONs with an average diameter of 5−10 nm, suspended in suitable carrier liquids (i.e., ferrofluids), show outstanding properties such as superparamagnetism. Superparamagnetism is obtained by nanoparticles that contain only a single magnetic domain. It is basically needed for biomedical applications, since, once the external magnetic field is removed, the magnetization disappears and thus the agglomeration and hence the possible embolization of the capillary vessels can be avoided (*42*, *56*, *69*, *100*, *106*). The excellent properties of SPIONs give rise to numerous multitask applications including MRI contrast agents (*42*, *107*), multimodal imaging (*85*), ferrofluid technology for thermotherapy (*69*, *108*), targeted drug delivery (*80*, *81*), cancer

DOI: 10.1021/cn100100e | *ACS Chem. Neurosci.* (2011), *2*, 118–140

Table 3. Toxicity Evaluation of SPIONs Using Various Methods

cytotoxicity evaluation method	shell composition	remarks	ref
MTT assay	PEG, PEGF, PVA, silica, dextran, PEI, and chitosan	No toxicity was observed even in the high applied dosage (about 1 mg/mL); a trace of toxicity was detected for bare SPIONs at the same concentrations.	(*98*, *104*, *122*−*127*)
modified MTT assay	PEGF and PVA	In order to reduce the effect of protein-nanoparticle interactions, surface saturated SPIONs were used; in this case the real toxicity of SPIONs was obtained.	(*101*, *102*)
redox assay	dextran, oleate, PL, and PEI	The SPIONs were stable in a variety of media and showed no toxicity during interactions with various cells.	(*128*−*130*)
cytochrome *c* assay	amine-functionalized	The results confirmed low cytotoxicity (LD_{50} 1500 μg/mL) of coated SPIONs on the liver cell (HepG2).	*131*
NBT assay	dextran	Results confirmed that dextran coated SPIONs did not significantly modify superoxide anion production compared to controls (human monocyte−macrophage).	*125*
WST assay	PDMAAm and dextran	No detectable cytotoxicity was observed on mesenchymal stem cells.	*132*
LDH assay	none	Bare SPIONs did not produce cytotoxicity up to a concentration of 100 μg/mL.	*133*
various dyes (e.g., NR and PI)	none, dextran, and PVA	No cytotoxicity, on cell-life cycle and apoptosis, was detected for the coated SPIONs; a trace of apoptosis was detected for the bare SPIONs at high concentrations (i.e., 80 mM).	(*105*, *121*, *134*)
cell cycle assay	none and PVA	PVA-coated SPION treated cells did not show evident necrosis, apoptosis, or cell cycle arrest in moderate concentration of nanoparticles (i.e., 200 mM); however, the coated nanoparticles at the highest concentration (400 mM) caused both apoptosis and cell cycle arrest in G_1 phase, possibly due to the irreversible DNA damage and repair of oxidative DNA lesions.	*99*
[^{3}H] thymidine incorporation assay	gold	No toxicity was detected on the employed concentrations (i.e., up to 30 μg/mL).	*79*
comet assay	none	Oxidative DNA lesions in cultured A549 cells after exposure to high concentrations of SPIONs (i.e., 40 μg/mL and 80 μg/mL) for 4 h showed enhancement in comparison with the control.	*113*

tumor detection via SQUID magnetometry (*109*), gene therapy (*56*), biomolecular separation (*110*), in vivo biomolecular detection (*85*), and tissue repair (*56*, *111*, *112*).

In order to enhance the biocompatibility of SPIONs, their surfaces have been covered by various biocompatible organic and inorganic materials (*81*, *93*). The obtained coated SPIONs could be functionalized and, consequently, could be tagged by active targeting moieties (e.g., antibodies) which leads to the enhancement of the targeting yield together with the reduction of patient resistance (*80*).

Cytotoxicity of SPIONs

Until now, most research on SPIONs has been dedicated to the synthesis, characterization, and surface properties of nanoparticles rather than to their biological issues (*99*). However, due to the increased presence of SPIONs in several branches of the medical sciences, together with the lack of cytotoxicity information, there are significant debates in the scientific community on their comprehensive toxicological evaluations. In recent years, the major focus of the published work in the field of SPIONs has been devoted to cytotoxicity evaluations (*86*, *93*, *98*, *99*, *113*).

The physicochemical properties of SPIONs (e.g., size and size distribution, shape, and surface characteristics) are of importance in terms of the corresponding biological responses (e.g., clearance, biodistribution, cell response/uptake, and cytotoxicity) (*114*). For instance, the bare particles are cleared from the blood due to their opsonization and corresponding clearance by the reticuloendothelial system (RES) (*80*); this clearance would be overcome by modifying the particles' surface using organic and inorganic materials (*93*). Besides opsonization, the sizes of the nanoparticles are recognized as being crucially important for their biodistribution; more specifically, SPIONs with a diameter below 10 nm would be removed rapidly through extravasation and renal clearance (*115*−*117*). Nanoparticles in a size range of 40−200 nm are taken by the liver (about 80%) and spleen (about 20%) (*95*, *118*). In order to increase the targeting capability of SPIONs, their residency time in the blood should be significantly enhanced; in this case, several amphiphilic materials (e.g., poly(ethylene glycol)) are used as coatings (*85*, *119*).

Due to the interaction of proteins with nanoparticles, the type of cell medium could have a significant effect on the obtained toxicity results of nanoparticles (*101*, *102*). In order to ascertain the cytotoxic characteristics of

DOI: 10.1021/cn100100e | *ACS Chem. Neurosci.* (2011), *2*, 118–140

SPIONs, their interaction with various cell types together with different cytotoxicity assays should be investigated (*120*). To achieve reliable toxicity results, the majority of conventional cytotoxicity protocols must be modified for nanoparticles. For instance, Mahmoudi and co-workers developed a new procedure (modified MTT) for evaluating the in vitro toxicity of SPIONs in a more rigorous manner, significantly improving the reliability of the obtained data (*101*, *102*).

In order to probe the possible cytotoxicity of both bare and coated SPIONs, extensive in vitro assays on various cell types and in vivo toxicity assays have been conducted (see Table 3). The results confirm that neither bare nor coated SPIONs have a detectable toxicity at applied dosages, which were greater than the dose permitted for humans (i.e., 0.56 mg/kg) by the U.S. Food and Drug Administration (*121*).

Role of SPIONs in MRI Imaging

SPIONs for Molecular Imaging

SPIONs have been used as contrast agents for MRI for at least two decades (*42*, *117*). Based on their size, SPIONs can be organized into several categories: (i) very small superparamagnetic iron oxide particles (VSPIONs, < 10 nm), (ii) ultrasmall superparamagnetic iron oxide particles (USPIONs, 10−50 nm), and (iii) standard superparamagnetic iron oxide particles (SPIONs, 50−180 nm) (*135*). SPIONs can be obtained using a wide range of synthetic approaches such as microemulsions, sol−gel synthesis, sonochemical reactions, hydrothermal reactions, hydrolysis and thermolysis of precursors, flow injection synthesis, and electrospray synthesis (*56*, *81*). The challenge is to produce monodisperse SPIONs with controllable size and shape in great quantities (*80*). One promising approach for large scale synthesis of SPIONs is the thermal decomposition of iron salts (*80*). SPIONs must be coated with surface complexing agents. After modification, it is necessary to prevent nanoparticle agglomeration, reduce toxicity, and obtain an adapted pharmacokinetics and biodistribution. It is also often desirable to select a surface coating with functional groups to allow the attachment of targeting ligands.

There are some prominent analytical techniques which are usually employed to characterize SPIONs, such as photon correlation spectroscopy (PCS), magnetometry, and relaxivity profiles (nuclear magnetic resonance dispersion (NMRD) curves) recorded over a wide range of magnetic fields. The PCS measurement gives a mean value of the hydrodynamic diameter of the particles. Magnetometry confirms the superparamagnetic property of the particle and provides information on the specific magnetization and the mean diameter of the crystals. The fitting of the NMRD curves according to the theories (*136*) gives the mean crystal size, the specific magnetization, and the Néel relaxation time (*137*). The nuclear magnetic relaxation properties of a compound are ideally obtained by the study of its NMRD profile, which gives the evolution of the relaxivity with respect to the external magnetic field. The relaxivity is defined as the increase of the relaxation rate of the solvent (water) induced by 1 mmol/L of the active ion. In the case of magnetite, the relaxivity is the relaxation rate enhancement observed for an aqueous solution containing 1 mmol Fe/L.

The ability of SPIONs to shorten the T_1 and T_2 proton relaxation times has been widely used to enhance the contrast of MR images. Clinical applications have been well differentiated: SPIONs are mainly used via intravenous infusion to detect and characterize small focal lesions in the liver (*138*−*140*). SPIONs can also be given orally to visualize the digestive tract. USPIONs have a longer plasmatic half-life (>36 h) and exhibit slower uptake by the liver and spleen after intravenous administration. This allows the product to access macrophages in normal (e.g., lymph nodes) or diseased tissue (e.g., MS, graft rejection, atheroma plaques, stroke, and rheumatoid arthritis) (*141*−*144*). They can also be used as biomarkers to evaluate the efficacy of treatments. Molecular imaging is an important new diagnostic tool for studying the in vivo cellular and molecular biology and allows for earlier disease detection. The field of molecular imaging is extending rapidly, and there are a number of interesting investigations being conducted using labeled SPIONs.

Many biomarkers of cancer have already been evaluated as targets for SPIONs (*145*−*147*). One example is the folate receptor which is overexpressed in many kinds of tumors including ovarian, breast, colorectal, renal cell carcinomas, brain metastases, or neuroendocrine cancers (*148*, *149*). This receptor is absent in most normal tissues. When folates were grafted on SPIONs, MRI showed an average intensity decrease of 38% within the tumor (*150*).

Another target is the transferrin receptor (TfR). A large number of studies have shown that elevated levels of TfR are often found on cancer cells compared with normal cells. Increased TfR expression has been found in breast cancer, bladder transitional cell carcinomas, prostate cancer, gliomas, or chronic lymphocytic leukemia (*151*, *152*). When human transferrin proteins coupled to SPIONs were injected in tumor-bearing mice, a 40% change in signal intensity was observed in T_2-weighted images (*153*). Many studies have already reported the ability of active targeting strategies to identify biomarkers of cardiovascular disease, inflammation, apoptosis, and other pathological conditions. Some examples are given in the following sections.

DOI: 10.1021/cn100100e | *ACS Chem. Neurosci.* (2011), *2*, 118–140

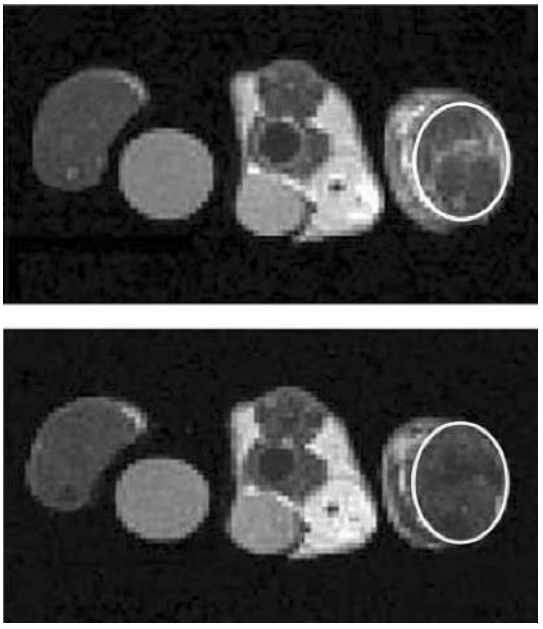

Figure 2. Effect of the USPIONs on the MR contrast in inflamed muscle. Typical T_2-weighted images before (top) and 3 h after (bottom) the administration of USPIO-PEGsLeX. The control muscle is located on the left, the inflamed muscle on the right. The white circles indicate the regions of interest in the inflamed muscles with an obvious signal decrease after administration of USPIO-PEG-sLeX. Reproduced with permission from ref *149*. Copyright 2000 Elsevier.

Molecular Imaging of Inflammation with SPIONs

During inflammation, cell adhesion molecules such as E-selectin are expressed on the endothelial cell surface. Radermacher et al. (*154*) have recently evaluated SPIONs grafted with a synthetic mimetic of sialyl Lewis-(x) (sLe(x)), a natural ligand of E-selectin expressed on leukocytes, for noninvasive diagnosis and monitoring of inflammation. The studies were conducted by MRI, thanks to the strong T_2 and T_2* effects of SPIONs, and by electron paramagnetic resonance (EPR), which offers the unique capability to quantify these particles. The mean iron oxide concentration in inflamed muscles after injection of grafted or ungrafted SPION particles was 0.8% and 0.4% of the initially injected dose, respectively. By EPR, the authors observed that the concentration of the grafted USPIO particles in inflamed muscles was twice higher than that of the ungrafted particles. Using MRI experiments, a higher signal loss was clearly observed in the inflamed muscle when grafted particles were injected in comparison with the ungrafted particles. Even taking into account a nonspecific accumulation of iron oxides, the targeting of SPION particles with E-selectin ligands significantly improved the sensitivity of detection of inflamed tissues (Figure 2).

The same mimetic was first used in vitro, on cultured human umbilical vein endothelial cells (HUVECs) stimulated to express inflammatory adhesion molecules, and in vivo, on a mouse model of hepatitis (*155*). In vitro results showed an extensive retention of SPIONs with sLe(x) on TNF-alpha stimulated HUVECs. Image intensity and R_2 measurements performed on T_2-weighted MRI demonstrated a significantly higher binding of SPION-sLe(x) on stimulated HUVECs. In vivo, SPIONs are known to pass through the fenestra of the liver and to be captured by Kupffer cells, inducing a loss of signal intensity on T_2-weighted images. Unexpectedly, when injected in Con A-treated mice, SPIONs-sLe(x) induced a significantly lower attenuation of liver signal intensity than that induced by SPIONs-sLe(x) injected in healthy mice or ungrafted SPION injected in Con A-treated mice. This suggested that the specific contrast media is retained extracellularly by an interaction with E-selectin overexpressed on the vascular endothelium (Figure 3). Boutry et al. (*155*) concluded that SPIONs grafted with sLe(x) are well suited for the MRI diagnosis of inflammation and for the in vitro evaluation of endothelial cell activation.

Another type of vectorized SPIONs, P904, was tested in a rabbit model of induced aortic atherosclerosis (*156*). In vivo angiography and T_2*-weighted plaque MR imaging were performed after administration of P904 and a reference-standard, ferumoxtran-10, in hyperlipidemic New Zealand white rabbits. With in vivo MR imaging, plaque analysis was possible as early as 24 h after P904 injection. The authors observed a 27.75% increase in vessel wall area due to susceptibility artifacts on day 2 and a 38.81% increase on day 3 after P904 administration, compared with a 44.5% increase in vessel wall area on day 7 and a 34.8% increase on day 10 after ferumoxtran-10 administration. These susceptibility artifacts were correlated with intraplaque iron uptake in the corresponding histological slices. Thus, SPIONs can be used for detection of vascular inflammation in atherosclerotic plaque.

Inflammation is an important component not only in autoimmune diseases but also in ischemic/degenerative disorders of the CNS. MRI allows visualization of neuroinflammation in vivo (*157*). SPIONs are phagocytosed by hematogenous macrophages upon systemic application into the circulation and allow, due to their paramagnetic effect, in vivo tracking by MRI of infiltration to the CNS in experimental CNS disorders, and also in MS and stroke. Targeting of inflammatory, activation-dependent enzymes such as myeloperoxidase or immune function molecules by MR contrast agents represents a molecular approach to visualize critical steps of lesion development caused by neuroinflammation. Clinical studies with Gd-DTPA in conjunction with experimental investigations, employing more sensitive contrast agents such as gadofluorine, revealed that breakdown of the blood-brain barrier and

DOI: 10.1021/cn100100e | *ACS Chem. Neurosci.* (2011), *2*, 118–140

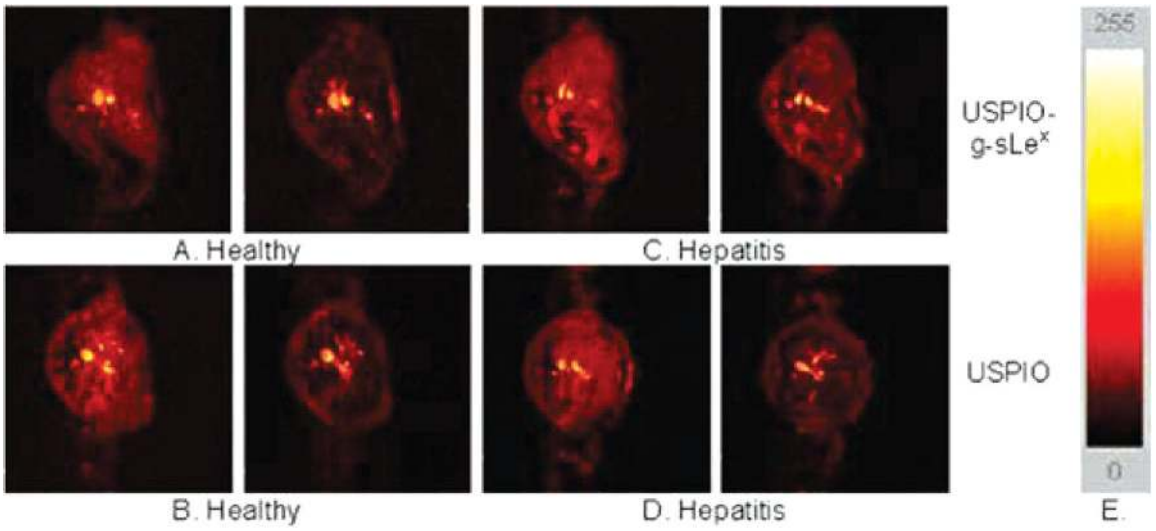

Figure 3. Axial GE MR images of healthy (A, B) and Con A-treated (C, D) mice 65 min after the injection of 30 mmol Fe/kg USPIONs (B, D) or USPIO-g-sLex (A, C). Color scale used for MR images shows signal intensity mapping with the Osiris software (E). Reproduced with permission from ref *150*. Copyright 2004 Elsevier.

SPION-related macrophage infiltration occur mostly independently. Cellular and targeted molecular MRI provides important insights into the dynamics of neuroinflammation. Considering the central role of inflammation in the pathophysiology of numerous disorders of the nervous system, it will be also pivotal for repair processes such as peripheral nerve regeneration. SPIONs are preferentially phagocytosed by monocytes before clearance within the reticuloendothelial system of the liver, spleen, and lymph nodes. Upon acute migration into the diseased nervous system, these iron-oxide-laden macrophages become visible in MRI due to the superparamagnetic effects of iron oxide which result in a signal loss on T_2-weighted and/or bright contrast on T_1-weighted images. SPIONs have allowed in vivo visualization of cellular inflammation during wallerian degeneration, experimental autoimmune neuritis and encephalomyelitis, and stroke in rodents, and also in patients with MS and stroke (*158*). Coupling of antibodies to SPIONs opens new avenues for molecular MRI and has been successfully used to visualize cell adhesion molecules guiding inflammation.

Nighoghossian and co-workers (*159*, *160*) showed that noninvasive imaging of inflammation associated with ischemic stroke lesions could have a predictive value and may be helpful for the development of cytoprotective drugs. In another study, Saleh et al. (*161*) determined the extent of SPION enhancement during the early stages of ischemic stroke. Parenchymal SPION enhancement occurred in three out of nine analyzed patients and was mainly evident on T_1-weighted spin−echo images. SPION dependent signal changes were spatially heterogeneous, reflecting the distinct patterns of hematogenous macrophage infiltration in different lesion types. Thus, SPION enhanced MRI may help to more specifically target anti-inflammatory therapy in patients with stroke.

SPION-laden macrophages can cause typical signal changes in the MRI of infarcted brain parenchyma, as demonstrated in studies of both experimental ischemia and human stroke (*162*). SPION-enhanced MRI may therefore represent an important tool to address, scientifically and clinically, the role of macrophages for ischemic lesion development.

Cengelli et al. (*163*) investigated the cellular uptake, cytotoxicity, and interaction of SPIONs (with various coatings including dextran, polyvinyl alcohol (PVA), amino-PVA, carboxylate-PVA, and thiol-PVA) with brain-derived endothelial cells, microglial cells, and differentiating three-dimensional aggregates. Due to their positive surface charge, amino-PVA coated SPIONs were taken up by isolated brain-derived endothelial and microglial cells at a much higher level than the other SPIONs; in addition, no inflammatory activation of these cells was detected. More specifically, amino-PVA coated SPIONs did not invade brain cell aggregates deeper than the first cell layer and did not induce inflammatory reaction in the aggregates. According to the obtained results, the positive-charged SPIONs are more biocompatible at applied dosage and would be more promising as vector systems for theragnostic applications in the brain, compared with the other tested nanoparticles (*163*).

SPIONs in Macrophage Imaging

A recent study evaluated macrophage imaging using SPIONs to depict bacterial knee infection in an experimental rabbit model. All inoculated knees presented

DOI: 10.1021/cn100100e | *ACS Chem. Neurosci.* (2011), *2*, 118–140

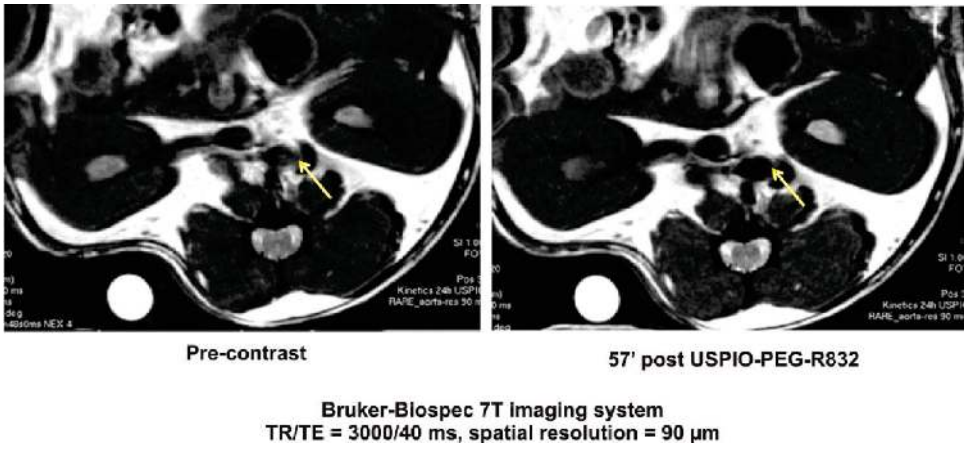

Figure 4. Development of a contrast agent for molecular diagnosis of atherosclerotic plaques (pre-clinical studies conducted on mice ApoE-/-); unpublished work by authors.

infectious synovitis with intense infiltration of iron-loaded macrophages. In these infected knees, signal loss was determined visually and quantitatively on T_1-weighted, T_2-weighted, and T_2*-weighted images, 24 h after SPION administration, reflecting the presence of SPION-loaded macrophages in the synovium. By comparison, no significant MR signal changes were observed in the control knees, which presented a normal synovium without infiltration of iron-loaded macrophages (*164*).

These researchers also evaluated SPION enhanced MR imaging for the differentiation of vertebral infectious osteomyelitis and sterile inflammation induced in two groups of six rabbits each. The MRI examinations performed included unenhanced and gadolinium-enhanced fat-saturated SE T_1-weighted sequences. Once end plate enhancement was observed on the T_1 gadolinium-enhanced MR sequence, a second MRI examination was performed 24 h after SPION administration. MRI was correlated with histopathological findings (*165*). On gadolinium-enhanced T_1 sequences, a significant increase in vertebral end plates was present in both groups without a significant difference between them. On SPION enhanced T_1 sequences, a significant SNR increase was observed only in the infection group with a significant difference in SNR between the infection and the sterile-inflammation groups. Infected areas presented replacement of bone marrow by an intense macrophage infiltration, with some being iron-loaded. Sterile inflammation showed a replacement of bone marrow by inflammatory tissue with only rare macrophages without any Perls' Prussian blue staining. SPION enhanced imaging can distinguish infectious osteomyelitis from sterile vertebral inflammation due to different macrophage distributions in the two lesions.

Because of their capability to secrete proteinases, macrophages play a central role in the growth and rupture of aneurysms. Noninvasive imaging of macrophages, therefore, may yield valuable information about the pathogenesis of aneurysm disease. Truijers et al. (*166*) studied the uptake of the macrophage-specific contrast agent SPIONs in the walls of aneurysms and normal-sized aortas. They showed that SPION uptake is limited or absent in the wall of normal-sized aortas and most aneurysms. However, individual abdominal aortic aneurysms exhibit high levels of SPION uptake, indicative of extensive macrophage infiltration in the aneurysm wall. Future research should focus on the predictive value of SPION uptake for the growth and rupture of aneurysms.

Kupffer cells play an important role in liver regeneration. Depression of Kupffer cell function is associated with poor outcome; however, there is no clinically safe and reliable method for evaluating their function. Saito et al. (*167*) evaluated Kupffer cell function in normal liver or in obstructive jaundice using magnetic resonance imaging following the injection of SPIONs, which are trapped by these cells. T_1-weighted signal intensity of the liver parenchyma was examined every 4 min for 60 min after SPION injection. The signal intensity values gradually decreased in both groups after accumulation of iron in the liver. Serum iron levels equally and significantly increased in both groups. By contrast, the values of relative enhancement, that is, percentage of signal intensity of precontrast to postcontrast, between 8 and 20 min after superparamagnetic iron oxide injection were significantly higher in the obstructive jaundice group than in the control, indicating Kupffer cell dysfunction in obstructive jaundiced liver. These results suggested that chronological magnetic resonance imaging with SPIONs is a suitable method for assessment of Kupffer cell function in patients with obstructive jaundice.

A number of research studies have shown the feasibility of in vivo MRI of rabbit atherosclerotic plaques with SPIONs (*168*−*170*). The uptake of SPIONs in the vessel wall of atherosclerotic rabbits led to strong focal signal loss in gradient echo images, while no effect in control animals was observed. Recently, our team has

DOI: 10.1021/cn100100e | *ACS Chem. Neurosci.* (2011), *2*, 118–140

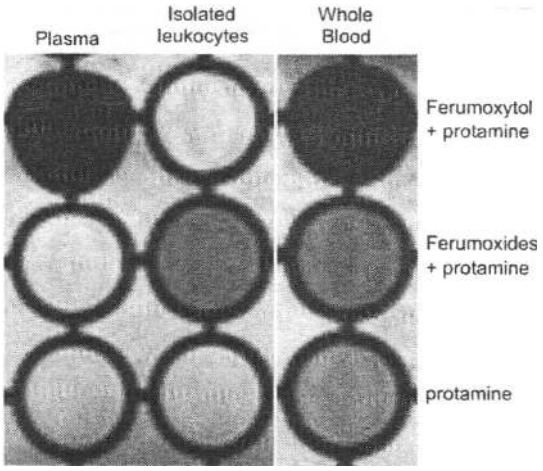

Figure 5. Evans rats received intravenous Fe-Pro complex, ferumoxytol (20 mg/kg)-Pro (2 mg/kg), or Pro alone. Whole blood, plasma, and mononuclear leukocytes were isolated after 2 h and transferred to a 96-well microtiter plate in 0.25% agarose. The presence of iron is indicated by a T_2 shortening effect (signal loss). Iron particles can be identified in the well containing isolated leukocytes after in vivo iron labeling with Fe-Pro complex but not after ferumoxtyol-Pro injection. Reproduced with permission from ref *116*. Copyright 1998 Informa Healthcare.

developed a new contrast agent for molecular diagnosis of atherosclerotic plaques. The peptide, selected by phage display (*209*), was grafted on the USPIO. This new nanosystem, USPIO-PEG-R832, was validated on HUVEC (Human Umbilical Vein Endothelial Cells) then by MRI, on mice Apo E-/- (see Figure 4).

SPIONs in Leukocyte Imaging

Cellular labeling with ferumoxide superparamagnetic iron oxide nanoparticles has been used to monitor cells in vivo by MRI (*120*). Long−Evans rats were intravenously injected with 20 mg/kg ferumoxides, ferumoxtran-10, or ferumoxytol, with or without protamine sulfate (Pro) (*121*). Leukocytes and splenocytes either were evaluated by cell sorting and iron histochemistry or were implanted into the brain for MRI. In comparison with ferumoxides or protamine sulfate alone, the injection of ferumoxides/protamine sulfate complex IV resulted in iron labeling of leukocytes. Cell sorting analysis indicated that iron-labeled cells were enriched for cell types positive for the myelomonocytic marker (CD11b/c) and the B lymphocyte marker (CD45RA) and depleted in the T cell marker (CD3). Neither ferumoxtran-10 nor ferumoxytol with protamine sulfate resulted in labeled leukocytes. In vivo ferumoxides/protamine-sulfate-loaded leukocytes were detected by MRI after intracerebral injection (Figure 5). The ferumoxides/protamine complex labeled CD45RA-positive and CD11b/c-positive leukocytes in vivo without immediate toxicity. The dose of ferumoxides used was much higher than the approved human dose, so additional animal studies are required before this approach can be clinically applied. These results might provide useful information for monitoring leukocyte trafficking into the brain.

Van Kasteren et al. (*171*) employed carbohydrate-functionalized SPIONs (i.e., MRI-visible glycol nanoparticles) which display multiple copies of the natural complex glycan, which is a ligand of selectins for the direct detection of endothelial markers E-/P-selectin (CD62E/CD62P) in acute brain diseases (see Figure 6). The developed glycol nanoparticles conjugated with sLe(x) have great potential for early detection of several catastrophic diseases such as MS, HIV, and Parkinson's (*171*−*177*).

Imaging Autoimmune Disorders with SPIONs

Autoimmune diseases are a heterogeneous class of diseases characterized by chronic inflammation of the target organ, often relapsing, invalidating, and requiring lifelong treatment. This process can occur years before the appearance of specific symptoms and can last for years after clinical diagnosis and the onset of treatment. Thus, once diagnosed, it is very important to try to achieve specific immune suppression with the aim of containing the disease, preventing or delaying complications, and avoiding relapse.

It has been possible to monitor distinct patterns of macrophage migration during the early stages of inflammation in a rodent model of chronic relapsing experimental autoimmune encephalomyelitis (EAE) (*178*). EAE inflammation processes are clearly linked to macrophage infiltration in the brain; a longitudinal protocol for macrophage visualization was designed, where SPIONs were injected repeatedly during the acute phase of the disease, the remitting phase, and the first relapse. SPION enhanced MRI and magnetization transfer ratios (MTRs) were used to assess blood-brain barrier (BBB) damage and neurological impairment as classical markers for CNS inflammation and tissue damage (Figure 7). During the acute phase, animals showed severe paralysis of the hind paws, intense accumulation of macrophages in brain tissue, and some diffuse patterns of BBB disruption. While SPION accumulation completely disappeared after the acute phase, residual damage of the BBB remained detectable in some lesions during the remitting phase. During the first relapse, the accumulation of SPION-loaded cells was less pronounced but still detectable. The time course of MTR, which is used as a marker for myelin loss, was linked to the infiltration of macrophages during the acute phase.

SPIONs as Theragnostic Agents for Multiple Sclerosis

Biocompatible SPIONs with suitable surface coatings (e.g., gold, silica, dextran, and poly(ethylene glycol)) (*80*, *93*) have been extensively employed for in vivo biomedical applications including MRI contrast enhancement (*179*, *180*), site specific release of drugs (*181*),

DOI: 10.1021/cn100100e | ACS Chem. Neurosci. (2011), 2, 118–140

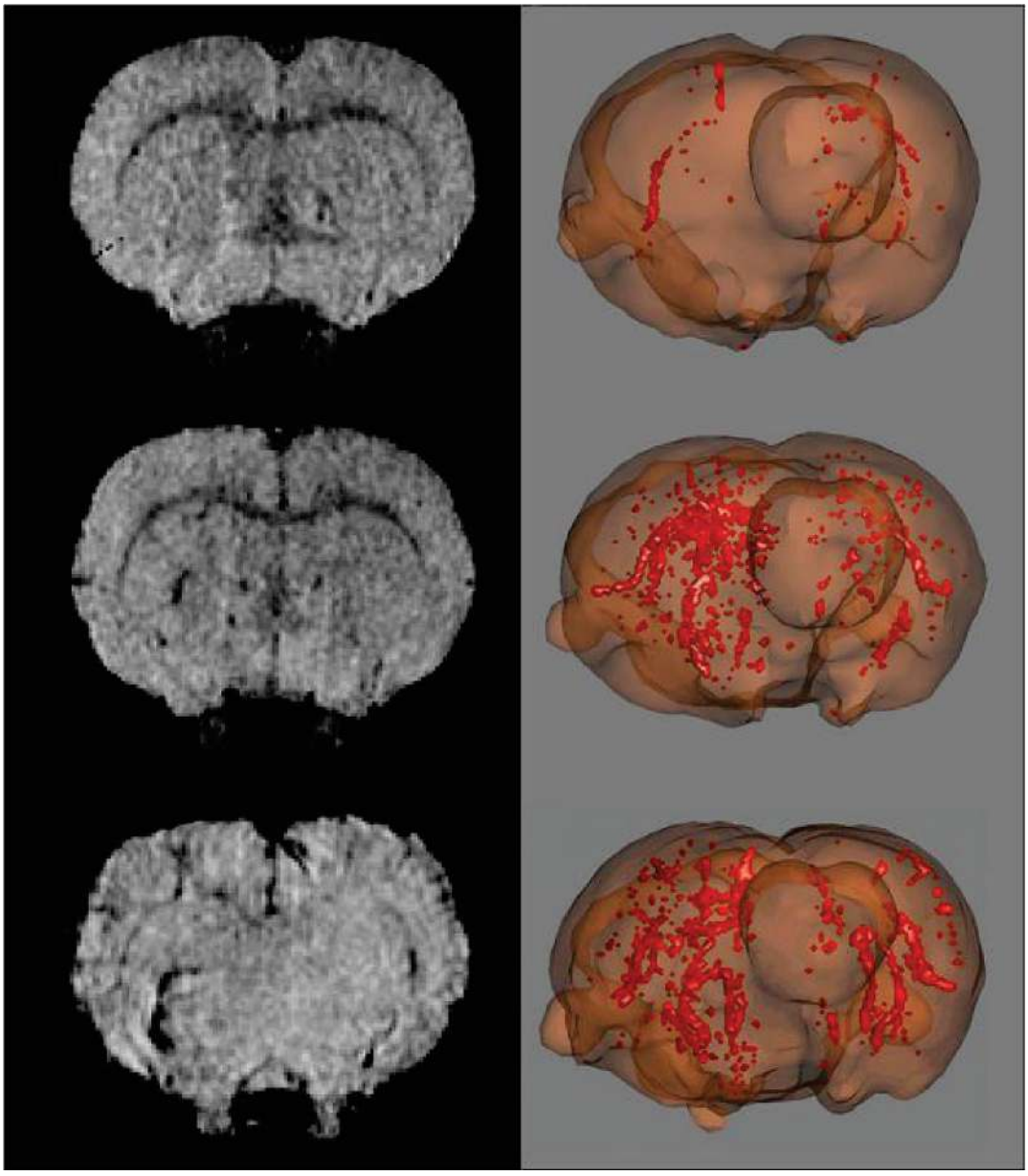

Figure 6. 3D data sets of T_2*-weighted images taken (A, C, and E) and 3D reconstructions of the accumulation of contrast agent (B, D, and F) reveal that glycol nanoparticles conjugated with sLe(x) enable clear detection of lesions in clinically relevant models of MS (C and D) and stroke (E and F) in contrast to unfunctionalized control nanoparticles (A and B). In addition, use of a gadolinium-based contrast agent in spin−echo T_1-weighted images to assess BBB permeability (G) and regional cerebral blood volume (H) failed to detect the presence of pathology. Views are from the front depicting left brain on the right-hand side. Reproduced with permission from ref *166*. Copyright 2009 American Roentgen Ray Society.

biomolecular imaging (*182*), hyperthermia (*108*), and magnetic field assisted radionuclide therapy (*183*). Some SPIONs with core sizes of 3−6 nm and dextran coating (with 20−150 nm hydrodynamic sizes), such as Feridex, are approved for MRI in patients (*184*, *185*). Correspondingly, drug-loaded SPIONs with shells of stimuli-sensitive polymers can potentially be guided to the desired target site using an external magnetic field or an existing conjugation of targeting species while simultaneously tracking the biodistribution of the nanoparticles (*186*). This approach truly makes them "theragnostic" (i.e., therapeutic and diagnostic), which has been comprehensively described in another review (*81*).

As mentioned previously, MS is a chronic autoimmune neurological disease (*187*) characterized by multifocal, relapsing-remitting symptoms related to CNS demyelination and neuronal injury or loss. Both genetic and environmental factors contribute to MS susceptibility (*188*−*190*).

DOI: 10.1021/cn100100e | *ACS Chem. Neurosci.* (2011), *2*, 118–140

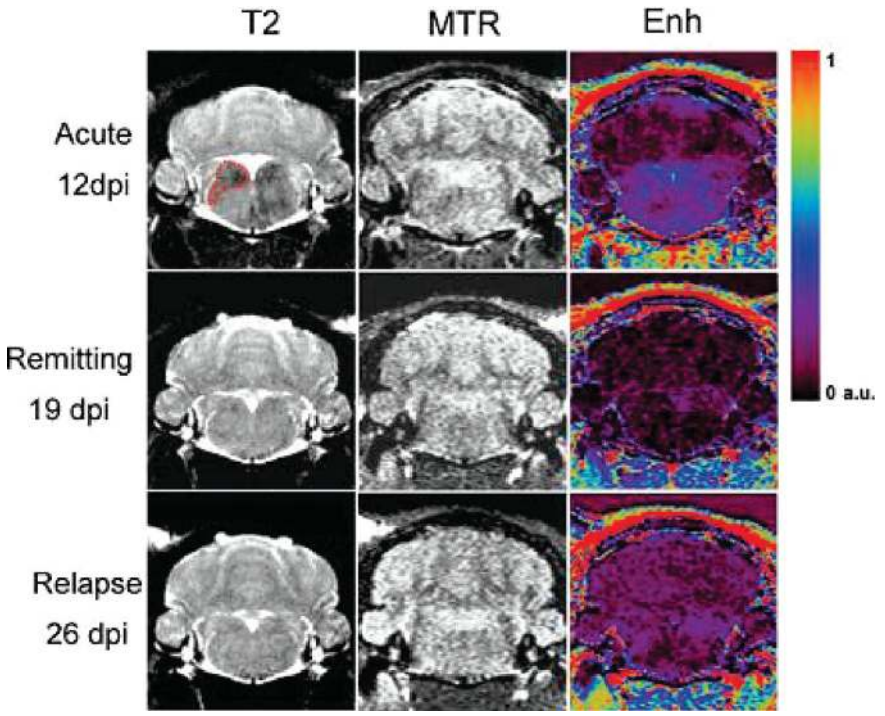

Figure 7. MRI brain scans of EAE animals during acute phase, i.e., 11, 12 dpi (first row), remitting phase 18, 19 dpi (second row), and first relapse 24, 25 dpi (third row). Left column: USPIONs enhancement. Tissue infiltrated by labeled macrophages appears hypointense in T_2-weighted images. Middle column: MTR maps. There are no large changes visible in the images. Right column: Enhancement of Gd-DOTA in brain tissue as a marker for BBB damage. Areas of Gd-DOTA extravasation in the medulla appear blue on the Enh maps. Enhancement of Gd-DOTA in the medulla is more diffuse as compared with USPIONs enhancement. Reproduced with permission from ref *173*. Copyright 2010 Informa Healthcare.

Proinflammatory M1 and immunomodulatory M2 activation profiles of circulating monocytes in a relapsing experimental autoimmune encephalomyelitis (EAE) model of MS have been investigated. Several approaches, including MRI macrophage tracking with SPIONs and expression patterns of M1/M2 macrophages and microglia in brain and M1/M2 monocytes in blood samples at various disease stages, have revealed that M1/M2 equilibrium in blood and CNS favors mild EAE, while an imbalance toward M1 promotes relapsing EAE. Accordingly, Mikita et al. (*191*) investigated whether M2 activated monocyte restoration in peripheral blood could cure acute clinical EAE. Administration of ex vivo activated M2 monocytes both suppressed ongoing severe EAE and increased immunomodulatory expression patterns in lesions, confirming their role in the induction of recovery. Imbalance of monocyte activation profiles and impaired M2 expression are key factors in the development of relapses.

Inflammatory MS lesions are characterized by microglia activation and infiltration of T cells, B cells, and macrophages across the blood-brain barrier (BBB). An earlier MR imaging investigation with a new contrast agent USPION that accumulates in phagocytic cells revealed the presence of macrophage brain infiltration in vivo. Twenty-four hours after injection, USPION uptake was observed in 33 acute MS lesions in 9 patients (*192*). Lesions were seen as high signal intensities on T_1-weighted images and low signal intensities on T_2-weighted images (Figure 8). Taken together with earlier findings obtained in experimental models or in human stroke, the visualization of macrophage activity in vivo with SPIONs characterizes a distinct cellular and inflammatory event of the dynamic process of MS lesion formation. The macrophage activity information obtained with SPIONs is distinct and complementary to the increased BBB permeability seen with gadolinium.

Using positron emission tomography (PET) and single photon emission computed tomography (SPECT), the radiotracer imaging method has been used for imaging of labeled immune cells (e.g., ^{68}Ga and ^{111}In) which cross the BBB and are retained in the CNS compartment (*193*, *194*). Very recently, SPIONs have been labeled with radiotracers (*183*, *195*), hence offering a great opportunity to probe MS with multimodal equipment (e.g., combination of MRI, PET, and SPECT) (*85*).

Vellinga et al. (*196*) showed that SPIONs could enhance brain MRI in MS showing patterns distinct from those with Gd-enhancement (see Figure 9). The obtained patterns provide complementary insight into the underlying pathology and are therefore clinically

DOI: 10.1021/cn100100e | *ACS Chem. Neurosci.* (2011), *2*, 118–140

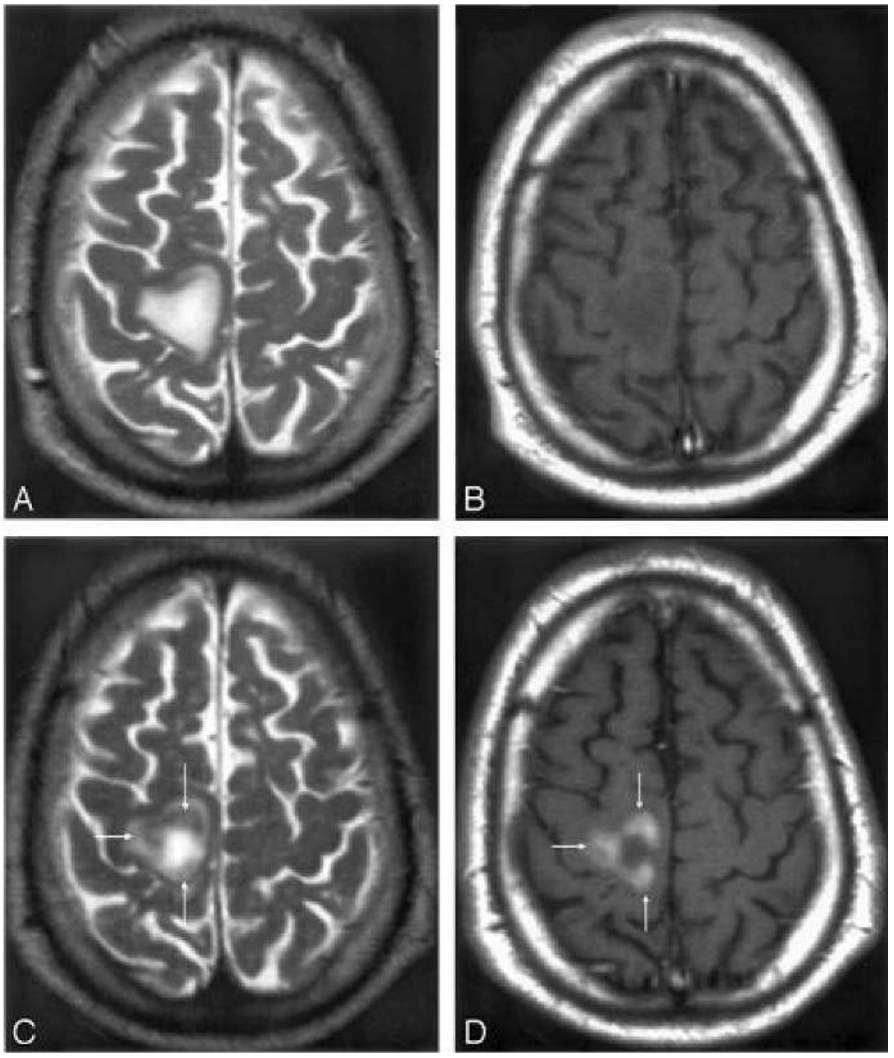

Figure 8. Mismatch of contrast agent uptake in a USPIONs-enhanced acute MS plaque. MR imaging 1 T_2-weighted image (A) and T_1-weighted postgadolinium image (B) show a large MS lesion that was not enhanced by gadolinium. MR imaging 2 shows the USPIONs uptake at the periphery of the lesion (arrows), seen as a decreased signal intensity on T_2-weighted images (C) and a high signal intensity on T_1-weighted images (D). Reproduced with permission from ref *179*. Copyright 2005 Wiley-Liss, Inc.

relevant as potential MRI markers for disease severity and possibly treatment efficacy.

Clinicians' Point of View

In the current clinical setup, the diagnosis of MS relies mainly on a clinical exacerbation compatible with MS and the finding of typical lesions on MRI. Clinical exacerbations and remissions are characteristics of MS. It is not clearly known why the disease shows activity in MRI with T2 lesions and gadolinium enhancing lesions in silent and/or eloquent regions of the brain and then goes into short- or long-term remission.

Several biomarkers have been reported for the diagnosis and detection of MS activity (*197*). Different types of biosensors are designed so that the presence of a biomarker of interest induces a detectable shift of the signal (e.g., change in mass, optical refractive index, or resonance frequency). It seems that nanotechnology is finding its way in detecting biomarkers in oncology, but little has been done for MS (*198*). If the changes before a relapse can be picked up at a proper time, then it will be possible to prevent the disease in a complete or partial way. SPION probes may help in detecting inflammatory invasion of activated immune cells into the central nervous system during their trafficking from the blood-brain barrier.

Once MS has been diagnosed, treating the disease mostly relies on applying disease modifying therapies and treatment of symptoms. Most of the approved drugs for MS focus on the inflammatory aspect of the disease and try to suppress or modify the immune system. The neurodegenerative aspect of the disease has been mentioned by different investigators; however,

DOI: 10.1021/cn100100e | *ACS Chem. Neurosci.* (2011), *2*, 118–140

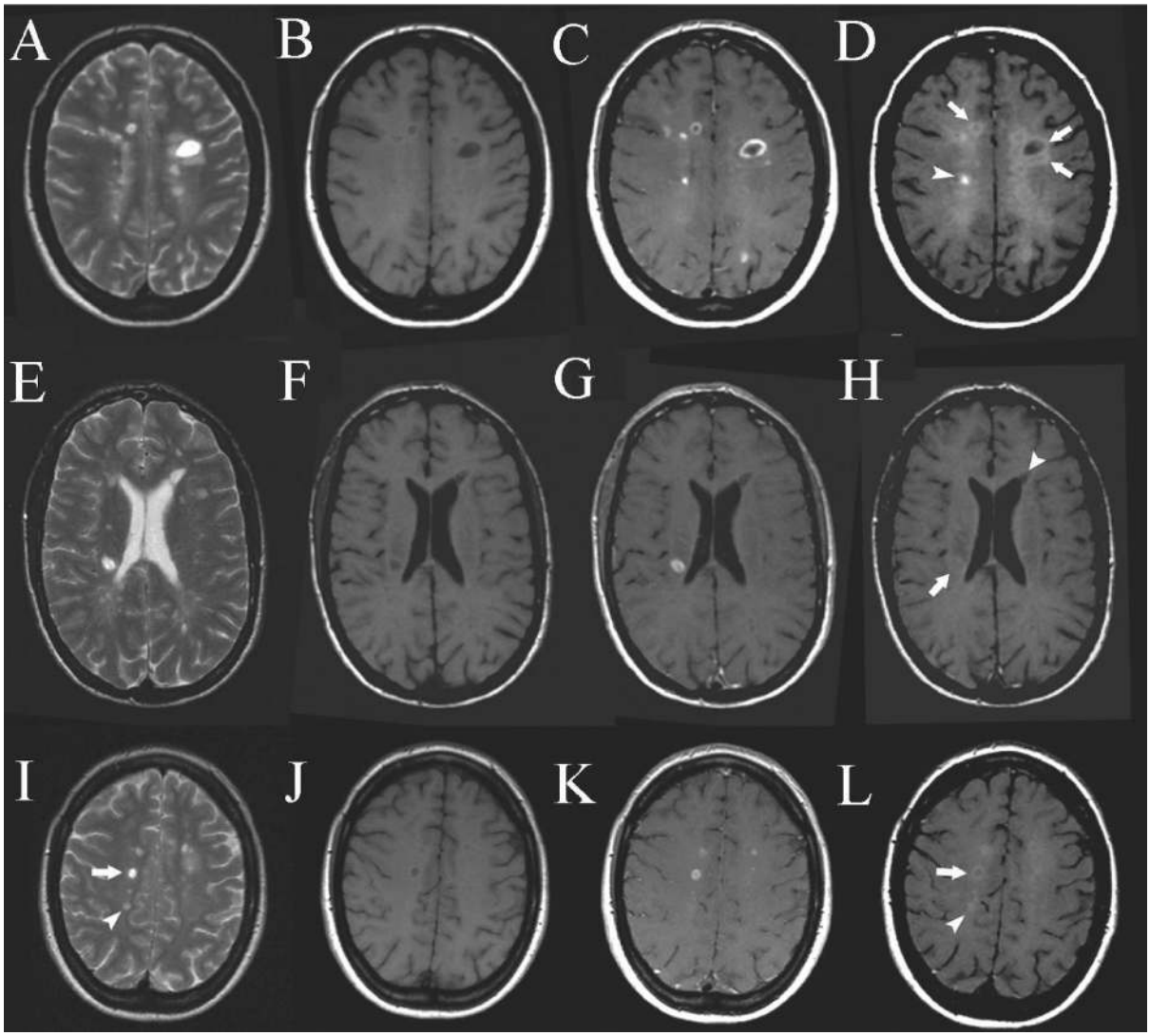

Figure 9. Cross-sectional patterns of lesion enhancement: pre-Gd T2SE images showing multiple periventricular MS lesions (A and E), pre-Gd T_1-weighted images showing hypointensity of some of the MS lesions (B and F), post-Gd T_1-weighted images showing several MS lesions enhanced with Gd in focal and ringlike patterns (C and G), post-USPIONs T_1-weighted images showing different patterns of USPIONs enhancement. Arrowhead upper row: focal USPIONs-enhancement. Arrows upper row: ringlike USPIONs-enhancement. Arrow bottom row: change to isointensity of a previously hypointense lesion as seen on precontrast T_1-weighted images (see B and F). Arrowhead bottom row: hypointense lesion that remains hypointense on post-USPIONs images (D and H). Pre-Gd T2SE images showing MS lesions (I), pre-Gd T_1-weighted images showing hypointensity of some of the MS lesions (J), some lesions are Gd-DTPA-positive (K), post-USPIONs images showing a Gd-DTPA-positive, USPIONs ring-enhancing lesion (arrow) and a Gd-DTPA-negative, focally USPIONs-positive lesion (arrowhead) (L). Reproduced with permission from ref *184*. Copyright 1999 Springer.

until now, there is no specific treatment for this aspect of MS (*199*). Many growth factors and neuropeptides are effective when administrated into the ventricle, but they lack efficiency for systematic application because of their failure to cross the BBB (*199*). Poly(ethylene glycol) (PEG)-coated nanoparticles have been successfully delivered into the brain and spinal cord in a rat model of experimental allergic encephalomyelitis (*200*). This gives hope that in the future more investigations will try to apply target specific agents in MS in a similar manner. Currently, nanodelivery of drugs into the brain is mainly used or investigated for brain tumors, but it can also be a major step forward for MS and other degenerative diseases.

Nanotechnologists' Point of View

The capability of SPIONs for tracking leukocyte migration in vivo can be very useful for studying brain inflammation in the early stages. More specifically, in MS disorder, SPIONs that are conjugated with targeting moieties together with the use of an external magnetic field can be a very promising alternative for simultaneous imaging of inflammation and drug delivery

DOI: 10.1021/cn100100e | *ACS Chem. Neurosci.* (2011), *2*, 118–140

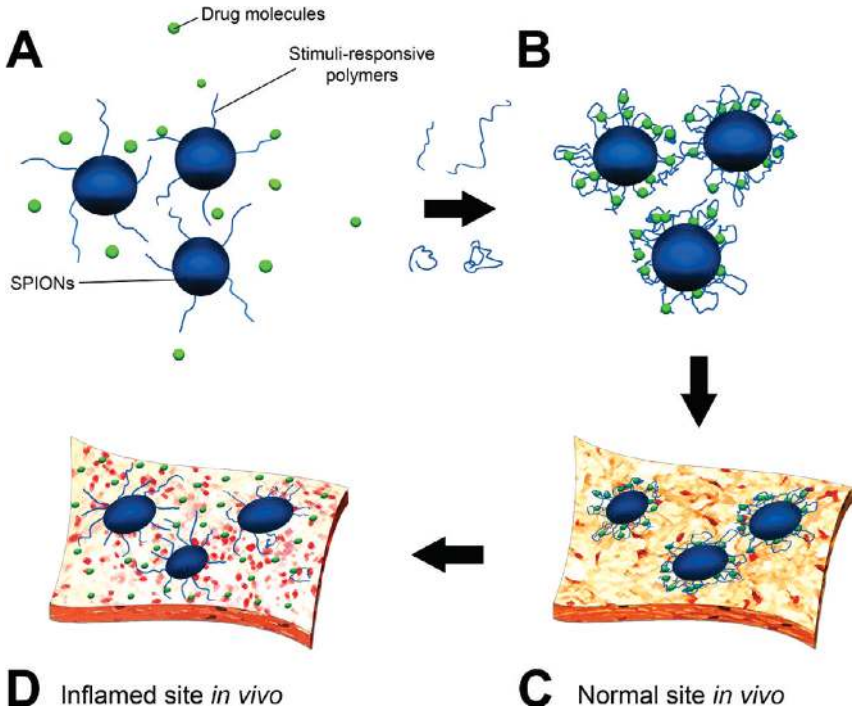

Figure 10. Cartoons of the loading/release function of future smart SPIONs for MS therapy, illustrating drug interaction with polymer brushes (A), trapping of drug using responsive behavior of polymer (B), and preservation and release of drug in the normal (C) and inflamed (D) sites due to the pH-responsive capability of polymer.

to inflammatory sites by maintaining appropriate local concentrations while reducing overall dosage and side effects (*201*). The future of MS theragnosis using nanoparticles, particularly using SPIONs, would be focused on multimodal nanoparticles. Radiotracers will be a good candidate to be trapped in the high density crystal lattice of the SPIONs for simultaneous monitoring, with various methods (e.g., MRI, PET, and SPECT), of the trafficking of immune system into the CNS. In order to increase the targeting yield of the multimodal SPIONs, their surfaces would be conjugated with various immune-specific targeting ligands, such as anti-E-selection antibody, anti-VCAM (i.e., vascular cell-adhesion molecule) antibody, and flumazanil targeting γ-aminobutyric acid$_A$ receptors (i.e., specific neurotransmitter receptors which are relevant to neuroimmune interaction or the progression of MS neuropathology) (*187*, *193*).

In addition to diagnosis, treatment could be achieved simultaneously by surface engineered SPIONs. In this case, the use of stimuli-responsive polymers on the surface of SPIONs would be vital. "Smart" SPIONs could be formed using stimuli-responsive polymers (e.g., poly(*N*-isopropylacrylamide) (*202*), triblock poly(styrene-*block*-2-vinylpyridine-*block*-ethylene oxide) (*203*), polystyrene-poly(methylmethacrylate) (*204*), polystyrene-poly(methylmethacrylate) (*205*), and poly(vinylmethylsiloxane) (*206*)) as coating on their surfaces. The conformation of these polymers can be changed with variations of surrounding environments (e.g., different dispersion solvents), regulation of the transport of ions and molecules, changing wettability and adhesion of different species on external stimuli, or conversion of chemical and biochemical signals into optical, electrical, thermal, and mechanical signals (*207*). Figure 10 shows the drug loading on the responsive polymer shell of the smart SPIONs and its release at inflamed sites. The suitable drug (e.g., interferon β-1a or interferon β-1b which are used to treat and control MS) (*208*) would be added to the aqueous colloidal dispersion of nanoparticles with brushed polymer chains on the surface of SPIONs; using suitable stimuli (e.g., medium pH enhancement), the polymer chains will be folded and the drug would be trapped on the folded chains. Using the various properties of the inflamed site in comparison with a normal tissue milieu (e.g., smaller amount of pH in the inflamed site), the smart SPIONs would have the capability to release the drugs in the inflamed site and not in the normal tissue.

Author Information

Corresponding Author

*E-mail: mahmoudi@biospion.com. Website: www.biospion.com.

References

1. Young, I. R., Hall, A. S., Pallis, C. A., Legg, N. J., Bydder, G. M., and Steiner, R. E. (1981) Nuclear magnetic

DOI: 10.1021/cn100100e | *ACS Chem. Neurosci.* (2011), *2*, 118–140

resonance imaging of the brain in multiple sclerosis. *Lancet 2*, 1063–1066.

2. Sahraian, M. A., and Eshaghi, A. (2010) Role of MRI in diagnosis and treatment of multiple sclerosis. *Clin. Neurol. Neurosurg. 112*, 609–615.

3. McDonald, W. I., Compston, A., Edan, G., Goodkin, D., Hartung, H. P., and Lublin, F. D. (2001) Recommended diagnostic criteria for multiple sclerosis: guidelines from the International Panel on the Diagnosis of Multiple Sclerosis. *Ann. Neurol. 50*, 121–127.

4. Polman, C. H., Reingold, S. C., Edan, G., Filippi, M., Hartung, H. P., and Kappos, L. (2005) Diagnostic criteria for multiple sclerosis: 2005 revisions to the "McDonald Criteria". *Ann. Neurol. 58*, 840–846.

5. Bakshi, R., Minagar, A., Jaisani, Z., and Wolinsky, J. S. (2005) Imaging of multiple sclerosis: role in neurotherapeutics. *NeuroRx 2*, 277–303.

6. Laule, C., Vavasour, I. M., and Whittall, K. P. (2003) Evolution of focal and diffuse magnetisation transfer abnormalities in multiple sclerosis. *J. Neurol. 250*, 924–931.

7. Trapp, B. D., and Nave, K. A. (2008) Multiple sclerosis: an immune or neurodegenerative disorder? *Annu. Rev. Neurosci. 31*, 247–269.

8. Rommer, P. S., and Stuve, O. (2008) Monoclonal antibodies in the therapy of multiple sclerosis. *J. Neurol. Suppl. 6*, 28–35.

9. Seigneuric, R., and Markey, L. (2010) From Nanotechnology to Nanomedicine: Applications to Cancer Research. *Curr. Mol. Med. 10*, 640–652.

10. Fang, C., and Zhang, M. (2010) Nanoparticle-based theragnostics: integrating diagnostic and therapeutic potentials in nanomedicine. *J. Controlled Release 146*, 2–5.

11. Lublin, F. (2005) History of modern multiple sclerosis therapy. *Neurology 252*, III/3–III/9.

12. Compston, A. (2005) *McAlpine's Multiple Sclerosis*, 4th ed., Churchill- Livingstone: New York.

13. Kabat, E. A., Moore, D. H., and Landow, H. (1942) An electrophoretic study of the protein components in cerebrospinal fluid and their relationship to the serum proteins. *J. Clin. Invest. 21*, 571–577.

14. Kurtzke, J. F. (1983) Rating neurologic impairment in multiple sclerosis: an expanded disability status scale (EDSS). *Neurology 33*, 1444–1452.

15. Filippini, G., Brusaferri, F., Sibley, W. A., Citterio, A., Ciucci, G., Midgard, R., and Candelise, L. (2000) Corticosteroids or ACTH for acute exacerbations in multiple sclerosis. *Cochrane Database Syst. Rev. 4*, xxx–xxx.

16. Bornstein, M. B., iller, A., Slagle, S., Weitzman, M., Crystal, H., Drexler, E., Keilson, M., Merriam, A., Wassertheil-Smoller, S., and Spada, V. (1987) A pilot trial of Cop 1 in exacerbating-remitting multiple sclerosis. *New Engl. J. Med. 317*, 408–414.

17. The IFNB Multiple Sclerosis Study Group (1993) Interferon beta-1b is effective in relapsing-remitting multiple sclerosis I Clinical results of a multicenter, randomized, double-blind, placebo-controlled trial. *Neurology 43*, 655–661.

18. The IFNB Multiple Sclerosis Study Group and the University of British Columbia MS/MRI Analysis Group (1995) Interferon beta-1b in the treatment of multiple sclerosis: final outcome of the randomised controlled trial. *Neurology 45*, 1277–1285.

19. Herndon, R. M., Richert, J. R., Salazar, A. M., Fischer, J. S., Goodkin, D. E., Granger, C. V., Simon, J. H., and Alam, J. J. (1996) Intramuscular interferon beta-1a for disease progression in relapsing multiple sclerosis. The Multiple Sclerosis Collaborative Research Group (MSCRG). *Ann. Neurol. 39*, 285–294.

20. Ford, C. C., Goldstein, J., Lisak, R. P., Myers, L. W., Panitch, H. S., Rose, J. W., and Schiffer, R. B. (1995) Copolymer 1 reduces relapse rate and improves disability in relapsing remitting multiple sclerosis: results of a phase III multicentre double-blind placebo-controlled trial. The Copolymer I Multiple Sclerosis Study Group. *Neurology 45*, 1268–1276.

21. PRISMS Study Group (1998) Randomized double-blind placebo-controlled study of interferon ss-1a in relapsing/remitting multiple sclerosis. *Lancet 352*, 1498–1504.

22. Hartung, H. P., Gonsette, R., and Konig, N. (2002) Mitoxantrone in progressive multiple sclerosis: a placebo-controlled, double-blind, randomised, multicentre trial. *Lancet 360*, 2018–2025.

23. Polman, H. M., Connor, P. O., and Havrdova, E. (2006) A Randomized, Placebo-Controlled Trial of Natalizumab for Relapsing Multiple Sclerosis. *N. Engl. J. Med. 354*, 899–910.

24. Kappos, L., Radue, E.-M., and O'Connor, P. (2010) A placebo-controlled trial of oral fingolimod in relapsing multiple sclerosis. *N. Engl. J. Med. 362*, 387–401.

25. www.mpikg-golm.mpg.de.

26. Brayner, R. (2008) The toxicological impact of nanoparticles. *Nano Today 3*, 48–55.

27. Maxwell, J. C. (1871) *Theory of Heat*, Dover Publications.

28. Zsigmondy, R. (1914) *Colloids and the Ultramicroscope*, J. Wiley and Sons, New York.

29. http://en.wikipedia.org/wiki/History_of_nanotechnology.

30. Zhang, L., and Webster, T. J. (2009) Nanotechnology and nanomaterials: Promises for improved tissue regeneration. *Nano Today 4*, 66–80.

31. http://en.wikipedia.org/wiki/William_McLellan_%28-nanotechnology%29.

32. Taniguchi, N., Proceedings of the International Conference on Precision Engineering (ICPE), Tokyo, Japan, 1974, pp 18−23.

33. Webster, T. J. (2007) *Int. J. Nanomed. 2*, 1.

34. http://en.wikipedia.org/wiki/Tom_Newman_%28scientist%29.

35. Thanh, N. T. K., and Green, L. A. W. (2010) Functionalisation of nanoparticles for biomedical applications. *Nano Today 5*, 213–230.

36. Fong, J., and Wood, F. (2006) Nanocrystalline silver dressings in wound management: a review. *Int. J. Nanomed. 1*, 441–449.

DOI: 10.1021/cn100100e | *ACS Chem. Neurosci.* (2011), *2*, 118–140

37. Takenaka, S., Karg, E., Roth, C., Schultz, H., Ziesenis, A., Heinzman, U., Schramel, P., and Heyder, J. (2001) Pulmonary and systemic distribution of inhaled ultrafine silver particles in rats. *Environ. Health Perspect. 109* (Suppl 4), 547–551.

38. Kang, S. J., Kim, B. M., Lee, Y. J., and Chung, H. W. (2008) Titanium dioxide nanoparticles trigger p53-mediated damage response in peripheral blood lymphocytes. *Environ. Mol. Mutagen. 49*, 399–405.

39. Kang, S. J., Kim, B. M., Lee, Y. J., Hong, S. H., and Chung, H. W. (2009) Titanium dioxide nanoparticles induce apoptosis through the JNK/p38-caspase-8-Bid pathway in phytohemagglutinin-stimulated human lymphocytes. *Biochem. Biophys. Res. Commun. 386*, 682–687.

40. Long, T. C., Saleh, N., Tilton, R. D., Lowry, G. V., and Veronesi, B. (2006) Titanium dioxide (P25) produces reactive oxygen species in immortalized brain microglia (BV2): Implications for nanoparticle neurotoxicity. *Environ. Sci. Technol. 40*, 4346–4352.

41. Dufour, E. K., Kumaravel, T., Nohynek, G. J., Kirkland, D., and Toutain, H. (2006) Clastogenicity, photoclastogenicity or pseudo-photo-clastogenicity: genotoxic effects of zinc oxide in the dark, in pre-irradiated or simultaneously irradiated Chinese hamster ovary cells. *Mutat. Res. 607*, 215–224.

42. Mahmoudi, M., Hosseinkhani, M., Boutry, S., Simchi, A., Hosseinkhani, H., Journeay, W. S., Subramani, K., and Laurent, S. (2011) MRI tracking of stem cells in vivo using iron oxide nanoparticles as a tool for the advancement of clinical regenerative medicine, *Chem. Rev.* In press. DOI: 10.1021/cr1001832.

43. Mahmoudi, M., Laurent, S., Azadmanesh, K., and Journeay, W. S. (2011) Effect of nanoparticles on cell-life cycle, *Chem. Rev.* In revision.

44. Shi, Y., Wang, F., He, J., Yadav, S., and Wamg, H. (2011) Titanium dioxide nanoparticles cause apoptosisin BEAS-2B cells through the caspase 8/t-Bid-independent mitochondrial pathway. *Toxicol. Lett. 196*, 21–27.

45. Theogaraj, E., Riley, S., Hughes, L., Maier, M., and Kirkland, D. (2007) An investigation of the photo-clastogenic potential of ultrafine titanium dioxide particles. *Mutat. Res. 634*, 205–219.

46. Warheit, D. B., Reed, K. L., and Webb, T. R. (2003) Pulmonary toxicity studies in rats with triethoxyoctylsilane (OTES)-coated pigment grade titanium dioxide particles: Bridging studies to predict inhalation hazard. *Exp. Lung Res. 29*, 593–606.

47. Xu, A., Chai, Y., and Hei, T. K. (2009) Genotoxic responses to titanium dioxide nanoparticles and fullerene in gpt delta transgenic MEF cells. *Part. Fibre Toxicol. 6*, 3.

48. Fiorito, S., Serafino, A., Andreola, F., and Bernier, P. (2006) Effects of fullerenes and single-wall carbon nanoubes on murine and human macrophages. *Carbon 44*, 1100–1105.

49. Gharbi, N., Pressac, M., Hadchouel, M., Szwarc, H., Wilson, S. R., and Moussa, F. (2005) [60] Fullerene is a powerful antioxidant in vivo with no acute or subacute toxicity. *Nano Lett. 5*, 2578–2585.

50. Jia, G., Wang, H., Yan, L., Wang, X., Pei, R., Yan, T., Zhao, Y., and Guo, X. (2005) Cytotoxicity of carbon nanomaterials: Single-wall nanotube, multi-wall nanotube and fullerene. *Environ. Sci. Technol. 39*, 1378–1383.

51. Bianco, A., Hoebeke, J., Godefroy, S., Chaloin, O., Pantarotto, D., Briand, J. P., Muller, S., Prato, M., and Partidos, C. D. (2005) Cationic carbon nanotubes bind to CpG oligodeoxynucleotides and enhance their immunostimulatory properties. *J. Am. Chem. Soc. 127*, 58–59.

52. Bianco, A., and Prato, M. (2003) Can carbon nanotubes be considered useful tools for biological applications? *Adv. Mater. 15*, 1765–1768.

53. Huczko, A., and Lange, H. (2001) Carbon nanotubes: experimental evidence for a null risk of skin irritation and allergy. *Fullerene Sci. Technol. 9*, 247–250.

54. Huczko, A., Lange, H., Calko, E., Grubek-Jaworksa, H., and Droszcz, P. (2001) Physiological testing of carbon nanotubes: Are they asbestos-like? *Fullerene Sci. Technol. 9*, 251–254.

55. Ying-ying, G., Tan Xiao-ping, T., Shu-quan, L., and Shang-bin, S. (2004) Effects of La3? doping on MnZn ferrite nanoscale particles synthesized by hydrothermal method. *J. Cent. South Univ. Technol. (Engl. Ed.) 11*, 113–228.

56. Laurent, S., Forge, D., Port, M., Roch, A., Robic, C., Vander Elst, L., and Muller, R. N. (2008) Magnetic iron oxide nanoparticles: Synthesis, stabilization, vectorization, physicochemical characterizations and biological applications. *Chem. Rev. 108*, 2064–2110.

57. Pollert, E., Veverka, P., Veverka, M., Kaman, O., Závěta, K., Vasseur, S., Epherre, R., Goglio, G., and Duguet, E. (2009) Search of new core materials for magnetic fluid hyperthermia: Preliminary chemical and physical issues. *Prog. Solid State Chem. 37*, 1–14.

58. Sawatzky, G. A., Van Der Woude, F., and Morrish, A. H. (1968) Cation distributions in octahedral and tetrahedral sites of the ferrimagnetic spinel $CoFe_2O_4$. *J. Appl. Phys. 39*, 1204–1205.

59. Brown, W. F. (1963) Thermal fluctuations of a single-domain particle. *Phys. Rev. 130*, 1677–1686.

60. Kuznetsov, O. A., Sorokina, O. N., Leontiev, V. G., Shlyakhtin, O. A., Kovarski, A. L., and Kuznetsov, A. A. (2007) ESR study of thermal demagnetization processes in ferromagnetic nanoparticles with Curie temperatures between 40 and 60 {ring operator} C. *J. Magn. Magn. Mater. 311*, 204–207.

61. Pollert, E. (1985) Crystal chemistry of magnetic oxides part 2: Hexagonal ferrites. *Prog. Cryst. Growth Charact. 11*, 155–205.

62. Auzans, E., Zins, D., Blums, E., and Massart, R. (1999) Synthesis and properties of Mn-Zn ferrite ferrofluids. *J. Mater. Sci. 34*, 1253–1260.

63. Sharma, R., and Chen, C. J. (2009) Newer nanoparticles in hyperthermia treatment and thermometry. *J. Nanopart. Res. 11*, 671–689.

64. Brusentsova, T. N., and Kuznetsov, V. D. (2007) Synthesis and investigation of magnetic properties of substituted

ferrite nanoparticles of spinel system $Mn_{1-x}Zn_x[Fe_{2-y}L_y]O_4$ *J. Magn. Magn. Mater. 311*, 22–25.

65. Sutariya, G. M., Vincent, D., Bayard, B., Upadhyay, R. V., Noyel, G., and Mehta, R. V. (2003) Magnetic DC field and temperature dependence on complex microwave magnetic permeability of ferrofluids: effect of constituent elements of substituted Mn ferrite. *J. Magn. Magn. Mater. 260*, 42–47.

66. Shuai, J., and Parker, I. (2005) Optical single-channel recording by imaging Ca^{2+} flux through individual ion channels: theoretical considerations and limits to resolution. *Cell Calcium 37*, 283–299.

67. Bretcanu, O., Verné, E., Cöisson, M., Tiberto, P., and Allia, P. (2006) Magnetic properties of the ferrimagnetic glass-ceramics for hyperthermia. *J. Magn. Magn. Mater. 305*, 529–533.

68. Weller, D., Moser, A., Folks, L., Best, M. E., Lee, W., Toney, M. F., and Schwickert, M. (2000) High ku materials approach to 100 gbits/in2. *IEEE Trans. Magn. 36*, 10–15.

69. Laurent, S. and Mahmoudi, M. (2010) Superparamagnetic Iron Oxide Nanoparticles for Hyperthermia, *Adv. Colloid Interface Sci*. Under review.

70. Casula, M. F., Floris, P., Innocenti, C., Lascialfari, A., Marinone, M., Corti, M., Sperling, R. A., Parak, W. J., and Sangregorio, C. (2010) Magnetic resonance imaging contrast agents based on iron oxide superparamagnetic ferrofluids. *Chem. Mater. 22*, 1739–1748.

71. Boni, A., Marinone, M., Innocenti, C., Sangregorio, C., Corti, M., Lascialfari, A., Mariani, M., Orsini, F., Poletti, G., and Casula, M. F. (2008) Magnetic and relaxometric properties of Mn ferrites. *J. Phys. D: Appl. Phys. 41*, 134021–134027.

72. Corti, M., Lascialfari, A., Micotti, E., Castellano, A., Donativi, M., Quarta, A., Cozzoli, P. D., Manna, L., Pellegrino, T., and Sangregorio, C. (2008) Magnetic properties of novel superparamagnetic MRI contrast agents based on colloidal nanocrystals. *J. Magn. Magn. Mater. 320*, e320–e323.

73. Berret, J.-F., Schonbeck, N., Gazeau, F., El Kharrat, D., Sandre, O., Vacher, A., and Airiau, M. (2006) Controlled Clustering of Superparamagnetic Nanoparticles Using Block Copolymers: Design of New Contrast Agents for Magnetic Resonance Imaging. *J. Am. Chem. Soc. 128*, 1755–1761.

74. Allemann, E., Leroux, J. C., and Gurny, R. (1998) Polymeric nano- and microparticles for the oral delivery of peptides and peptidomimetics. *Adv. Drug Delivery Rev. 34*, 171–189.

75. Constantinides, P. P., Chaubal, M. V., and Shorr, R. (2008) Advances in lipid nanodispersions for parenteral drug delivery and targeting. *Adv. Drug Delivery Rev. 60*, 757–767.

76. Hamidi, M., Azadi, A., and Rafiei, P. (2008) Hydrogel nanoparticles in drug delivery. *Adv. Drug Delivery Rev. 60*, 1638–1649.

77. Matsumura, Y. (2008) Poly(amino acid) micelle nanocarriers in preclinical and clinical studies. *Adv. Drug Delivery Rev. 60*, 899–914.

78. Otsuka, H., Nagasaki, Y., and Kataoka, K. (2003) PEGylated nanoparticles for biological and pharmaceutical applications. *Adv. Drug Delivery Rev. 55*, 403–419.

79. Kamei, K., Mukai, Y., Kojima, H., Yoshikawa, T., Yoshikawa, M., Kiyohara, G., Yamamoto, T. A., Yoshioka, Y., Okada, N., Seino, S., and Nakagawa, S. (2009) Direct cell entry of gold/iron-oxide magnetic nanoparticles in adenovirus mediated gene delivery. *Biomaterials 30*, 1809–1814.

80. Mahmoudi, M., Milani, A. S., and Stroeve, P. (2010) Surface Architecture of Superparamagnetic Iron Oxide Nanoparticles for Application in Drug Delivery and Their Biological Response: A Review. *Int. J. Biomed. Nanosci. Nanotechnol. 1*, 164–201.

81. Mahmoudi, M., Sant, S., Wang, B., Laurent, S., and Sen, T. (2011) Superparamagnetic iron oxide nanoparticles (SPIONs): Development, surface modification and applications in chemotherapy, *Adv. Drug Delivery Rev*. In press. DOI: 10.1016/j.addr.2010.05.006.

82. Ge, J., Hu, Y., Biasini, M., Beyermann, W. P., and Yin, Y. (2007) Superparamagnetic Magnetite Colloidal Nanocrystal Clusters. *Angew. Chem. 119*, 4420–4423.

83. Ge, J., Hu, Y., and Yin, Y. (2007) Highly Tunable Superparamagnetic Colloidal Photonic Crystals. *Angew. Chem., Int. Ed. 46*, 7428 –7431.

84. Nel, A. E., Madler, L., Velegol, D., Xia, T., Hoek, E. M. V., Somasundaran, P., Klaessig, F., Castranova, V., and Thompson, M. (2009) understanding biophysicochemical interactions at the nano−bio interface. *Nat. Mater. 8*, 543–557.

85. Mahmoudi, M., Serpooshan, V., Laurent, S. (2011) Engineered nanoparticles for biomolecular imaging, *Nanomedicine*, in revision.

86. Mahmoudi, M., Simchi, A., Imani, M., and Hafeli, U. O. (2009) Superparamagnetic iron oxide nanoparticles with rigid cross-linked polyethylene glycol fumarate coating for application in imaging and drug delivery. *J. Phys. Chem. C 113*, 8124–8131.

87. Arbab, A. S., Bashaw, L. A., Miller, B. R., Jordan, E. K., Lewis, B. K., Kalish, H., and Frank, J. A. (2003) Characterization of Biophysical and Metabolic Properties of Cells Labeled with Superparamagnetic Iron Oxide Nanoparticles and Transfection Agent for Cellular MR Imaging. *Radiology 229*, 838–846.

88. Foote, R. S., Lee, J. W., Jin, S., Leach, J. C., Ye, K. (2009) Nanoparticle-Mediated Gene Delivery, in *Micro and Nano Technologies in Bioanalysis*, pp 547−557, Humana Press.

89. Ito, A., Takizawa, Y., Honda, H., Hata, K., Kagami, H., Ueda, M., and Kobayashi, T. (2004) Tissue engineering using magnetite nanoparticles and magnetic force: heterotypic layers of cocultured hepatocytes and endothelial cells. *Tissue Eng. 10*, 833–840.

90. US demand for nanotechnologymedical products to approach $53 billion in 2011−Report. nanotechwire.com [online News Release] 2007 March 16, 2007 [cited July 3, 2008]; available from http://nanotechwire.com/news.asp?nid=4446.

91. Jones, C. F., and Grainger, D. W. (2009) In vitro assessments of nanomaterial toxicity. *Adv. Drug Delivery Rev. 61*, 438–456.

DOI: 10.1021/cn100100e | *ACS Chem. Neurosci.* (2011), *2*, 118–140

92. Aillon, K. L., Xie, Y., El-Gendy, N., Berkland, C. J., and Forrest, M. L. (2009) Effects of nanomaterial physicochemical properties on in vivo toxicity. *Adv. Drug Delivery Rev. 61*, 457–466.

93. Mahmoudi, M., Simchi, A., and Imani, M. (2010) Recent Advances in Surface Engineering of Superparamagnetic Iron Oxide Nanoparticles for Biomedical Applications. *J. Iran. Chem. Soc. 7*, S1–S27.

94. Gao, J., and Xu, B. (2009) Applications of nanomaterials inside cells. *Nano Today 4*, xxx–xxx.

95. Arruebo, M., Fernádez-Pacheco, R., Ibarra, M. R., and Santamaría, J. (2007) Magnetic nanoparticles for drug delivery. *Nano Today 2*, 22–32.

96. Laurent, S., Bridot, J. L., Vander Elst, L., and Muller, R. (2010) Magnetic iron oxide nanoparticles for biomedical applications. *Future Med. Chem. 2*, 427–449.

97. Mahmoudi, M., Sardari, S., Shokrgozar, M. A., Laurent, S., and Stroeve, P. (2011) Interaction of superparamagnetic iron oxide nanoparticles with human transferrin: Irreversible changes in human transferrin conformation, *Nanoscale*, In press. DOI: 10.1039/c0nr00733a.

98. Mahmoudi, M., Shokrgozar, M. A., Simchi, A., Imani, M., Milani, A. S., Stroeve, P., Vali, H., Hafeli, U. O., and Bonakdar, S. (2009) Multiphysics flow modeling and in vitro toxicity of iron oxide nanoparticles coated with poly(vinyl alcohol). *J. Phys. Chem. C 113*, 2322–2331.

99. Mahmoudi, M., Simchi, A., and Imani, M. (2009) Cytotoxicity of uncoated and polyvinyl alcohol coated superparamagnetic iron oxide nanoparticles. *J. Phys. Chem. C 113*, 9573–9580.

100. Mahmoudi, M., Simchi, A., Imani, M., Milani, A. S., and Stroeve, P. (2008) Optimal design and characterization of superparamagnetic iron oxide nanoparticles coated with polyvinyl alcohol for targeted delivery and imaging. *J. Phys. Chem. B 112*, 14470–14481.

101. Mahmoudi, M., Simchi, A., Imani, M., Milani, A. S., and Stroeve, P. (2009) An in vitro study of bare and poly(ethylene glycol)-co-fumarate-coated superparamagnetic iron oxide nanoparticles: A new toxicity identification procedure. *Nanotechnology 20*, 225104.

102. Mahmoudi, M., Simchi, A., Imani, M., Shokrgozar, M. A., Milani, A. S., Hafeli, U. O., and Stroeve, P. (2010) A new approach for the in vitro identification of the cytotoxicity of superparamagnetic iron oxide nanoparticles. *Colloids Surf., B 75*, 300–309.

103. Mahmoudi, M., Simchi, A., Imani, M., Stroeve, P., and Sohrabi, A. (2010) Templated growth of superparamagnetic iron oxide nanoparticles by temperature programming in the presence of poly(vinyl alcohol). *Thin Solid Films 518*, 4281–4289.

104. Mahmoudi, M., Simchi, A., Milani, A. S., and Stroeve, P. (2009) Cell toxicity of superparamagnetic iron oxide nanoparticles. *J. Colloid Interface Sci. 336*, 510–518.

105. Mahmoudi, M., Simchi, A., Vali, H., Imani, M., Shokrgozar, M. A., Azadmanesh, K., and Azari, F. (2009) Cytotoxicity and cell cycle effects of bare and poly(vinyl alcohol)-coated iron oxide nanoparticles in mouse fibroblasts. *Adv. Eng. Mater. 11*, B243–B250.

106. Papaefthymiou, G. C. (2009) Nanoparticle magnetism. *Nano Today 4*, 438–447.

107. Kohler, N., Fryxell, G. E., and Zhang, M. (2004) A bifunctional poly(ethylene glycol) silane immobilized on metallic oxide-based nanoparticles for conjugation with cell targeting agents. *J. Am. Chem. Soc. 126*, 7206–7211.

108. Reinl, H. M., Peller, M., Hagmann, M., Turner, P., Issels, R. D., and Reiser, M. (2005) Ferrite-enhanced MRI monitoring in hyperthermia. *J. Magn. Reson. Imaging 23*, 1017–1020.

109. Shultz, M. D., Ulises Reveles, J., Khanna, S. N., and Carpenter, E. E. (2007) Reactive nature of dopamine as a surface functionalization agent in iron oxide nanoparticles. *J. Am. Chem. Soc. 129*, 2482–2487.

110. Wang, D., He, J., Rosenzweig, N., and Rosenzweig, Z. (2004) Superparamagnetic Fe2O3 beads-CdSe/ZnS quantum dots core-shell nanocomposite particles for cell separation. *Nano Lett. 4*, 409–413.

111. Gupta, A. K., Naregalkar, R. R., Vaidya, V. D., and Gupta, M. (2007) Recent advances on surface engineering of magnetic iron oxide nanoparticles and their biomedical applications. *Nanomedicine 2*, 23–39.

112. Gupta, A. K., and Gupta, M. (2005) Synthesis and surface engineering of iron oxide nanoparticles for biomedical applications. *Biomaterials 26*, 3995–4021.

113. Karlsson, H. L., Cronholm, P., Gustafsson, J., and Muller, L. (2008) Copper oxide nanoparticles are highly toxic: A comparison between metal oxide nanoparticles and carbon nanotubes. *Chem. Res. Toxicol. 21*, 1726–1732.

114. Thorek, D. L. J., Chen, A. K., Czupryna, J., and Tsourkas, A. (2006) Superparamagnetic iron oxide nanoparticle probes for molecular imaging. *Ann. Biomed. Eng. 34*, 23–38.

115. Lu, J., Yang, S., Ng, K. M., Su, C. H., Yeh, C. S., Wu, Y. N., and Shieh, D. B. (2006) Solid-state synthesis of monocrystalline iron oxide nanoparticle based ferrofluid suitable for magnetic resonance imaging contrast application. *Nanotechnology 17*, 5812–5820.

116. Bonnemain, B. (1998) Superparamagnetic agents in magnetic resonance imaging: Physicochemical characteristics and clinical applications. A review. *J. Drug Targeting 6*, 167–174.

117. Weissleder, R., Elizondo, G., Wittenberg, J., Rabito, C. A., Bengele, H. H., and Josephson, L. (1990) Ultrasmall superparamagnetic iron oxide: Characterization of a new class of contrast agents for MR imaging. *Radiology 175*, 489–493.

118. Mornet, S., Vasseur, S., Grasset, F., and Duguet, E. (2004) Magnetic nanoparticle design for medical diagnosis and therapy. *J. Mater. Chem. 14*, 2161–2175.

119. Passirani, C., Barratt, G., Devissaguet, J. P., and Labarre, D. (1998) Long-circulating nanoparticles bearing heparin or dextran covalently bound to poly(methyl methacrylate). *Pharm. Res. 15*, 1046–1050.

120. Soenen, S. J. H., and De Cuyper, M. (2009) Assessing cytotoxicity of (iron oxide-based) nanoparticles: An overview of different methods exemplified with cationic magnetoliposomes. *Contrast Media Mol. Imaging 4*, 207–219.

121. Wu, Y. J., Muldoon, L. L., Varallyay, C., Markwardt, S., Jones, R. E., and Neuwelt, E. A. (2007) In vivo leukocyte labeling with intravenous ferumoxides/protamine sulfate complex and in vitro characterization for cellular magnetic resonance imaging. *Am. J. Physiol. 293*, C1698–C1708.

122. Gupta, A. K., Berry, C., Gupta, M., and Curtis, A. (2003) Receptor-mediated targeting of magnetic nanoparticles using insulin as a surface ligand to prevent endocytosis. *IEEE Tran. Nanobiosci. 2*, 255–261.

123. Gupta, A. K., and Wells, S. (2004) Surface-Modified Superparamagnetic Nanoparticles for Drug Delivery: Preparation, Characterization, and Cytotoxicity Studies. *IEEE Trans. Nanobiosci. 3*, 66–73.

124. Kim, J. S., Yoon, T. J., Yu, K. N., Mi, S. N., Woo, M., Kim, B. G., Lee, K. H., Sohn, B. H., Park, S. B., Lee, J. K., and Cho, M. H. (2006) Cellular uptake of magnetic nanoparticle is mediated through energy-dependent endocytosis in A549 cells. *J. Vet. Sci. 7*, 321–326.

125. Muller, K., Skepper, J. N., Posfai, M., Trivedi, R., Howarth, S., Corot, C., Lancelot, E., Thompson, P. W., Brown, A. P., and Gillard, J. H. (2007) Effect of ultrasmall superparamagnetic iron oxide nanoparticles (Ferumoxtran-10) on human monocyte-macrophages in vitro. *Biomaterials 28*, 1629–1642.

126. Mykhaylyk, O., Antequera, Y. S., Vlaskou, D., and Plank, C. (2007) Generation of magnetic nonviral gene transfer agents and magnetofection in vitro. *Nat. Protoc. 2*, 2391–2411.

127. Ge, Y., Zhang, Y., He, S., Nie, F., Teng, G., and Gu, N. (2009) Fluorescence modified chitosan-coated magnetic nanoparticles for high-efficient cellular imaging. *Nanoscale Res. Lett. 4*, 287–295.

128. Farrell, E., Wielopolski, P., Pavljasevic, P., Kops, N., Weinans, H., Bernsen, M. R., and van Osch, G. J. V. M. (2009) Cell labelling with superparamagnetic iron oxide has no effect on chondrocyte behaviour. *Osteoarthritis Cartilage 17*, 958–964.

129. Chorny, M., Polyak, B., Alferiev, I. S., Walsh, K., Friedman, G., and Levy, R. J. (2007) Magnetically driven plasmid DNA delivery with biodegradable polymeric nanoparticles. *FASEB J. 21*, 2510–2519.

130. Samanta, B., Yan, H., Fischer, N. O., Shi, J., Jerry, D. J., and Rotello, V. M. (2008) Protein-passivated Fe_3O_4 nanoparticles: Low toxicity and rapid heating for thermal therapy. *J. Mater. Chem. 18*, 1204–1208.

131. Huang, G., Diakur, J., Xu, Z., and Wiebe, L. I. (2008) Asialoglycoprotein receptor-targeted superparamagnetic iron oxide nanoparticles. *Int. J. Pharm. 360*, 197–203.

132. Babic, M., Horok, D., Jendelová, P., Glogarová, K., Herynek, V., Trchova, M., Likavoanová, K., Lesny, P., Pollert, E., Hajek, M., and Sykova, E. (2009) Poly(*N*,*N*-dimethylacrylamide)-coated maghemite nanoparticles for stem cell labeling. *Bioconjugate Chem. 20*, 283–294.

133. Hussain, S. M., Hess, K. L., Gearhart, J. M., Geiss, K. T., and Schlager, J. J. (2005) In vitro toxicity of nanoparticles in BRL 3A rat liver cells. *Toxicol. in Vitro 19*, 975–983.

134. Pawelczyk, E., Arbab, A. S., Chaudhry, A., Balakumaran, A., Robey, P. G., and Frank, J. A. (2008) In vitro model of bromodeoxyuridine or iron oxide nanoparticle uptake by activated macrophages from labeled stem cells: Implications for cellular therapy. *Stem Cells 26*, 1366–1375.

135. Corot, C., Robert, P., Idée, J. M., and Port, M. (2006) Recent advances in iron oxide nanocrystal technology for medical imaging. *Adv. Drug Delivery Rev. 58*, 1471–1504.

136. Muller, R. N., Roch, A., Colet, J. M., Ouakssim, A., and Gillis, P. (2001) Particulate magnetic contrast agents, in *The chemistry of contrast agents in medical magnetic resonance imaging* (Merbach, A.E. and Toth, E., Eds.), Chapter 10, pp 417−435, Wiley.

137. Ouakssim, A., Fastrez, S., Roch, A., Laurent, S., Gossuin, Y., Pierart, C., Vander Elst, L., and Muller, R. N. (2004) Control of the synthesis of magnetic fluids by relaxometry and magnetometry. *J. Magn. Magn. Mater. 272−276*, e1711–e1713.

138. Sofue, K., Tsurusaki, M., Miyake, M., Sakurada, A., Arai, Y., and Sugimura, K. (2010) Detection of hepatic metastases by superparamagnetic iron oxide-enhanced MR imaging: prospective comparison between 1.5-T and 3.0-T images in the same patients, *Eur. Radiol.* In press.

139. Zhang, J. X., Dang, S. C., Zhang, Y., Sha, X., Zhang, L. R., Wei, C. S., Chen, M., and Jiang, D. L. (2010) MRI shows clodronate-liposomes attenuating liver injury in rats with severe acute pancreatitis. *Hepatobiliary Pancreat Dis. Int. 9*, 192–200.

140. Zhou, B., Shan, H., Li, D., Jiang, Z. B., Qian, J. S., Zhu, K. S., Huang, M. S., and Meng, X. C. (2010) MR tracking of magnetically labeled mesenchymal stem cells in rats with liver fibrosis. *J. Magn. Reson. Imaging 28*, 394–399.

141. Vellinga, M. M., Vrenken, H., Hulst, H. E., Polman, C. H., Uitdehaag, B. M., Pouwels, P. J., Barkhof, F., and Geurts, J. J. (2009) Use of ultrasmall superparamagnetic particles of iron oxide (USPIO)-enhanced MRI to demonstrate diffuse inflammation in the normal-appearing white matter (NAWM) of multiple sclerosis (MS) patients: an exploratory study. *J. Magn. Reson. Imaging 29*, 774–779.

142. Stoll, G., and Bendszus, M. (2010) New approaches to neuroimaging of central nervous system inflammation. *Curr. Opin. Neurol. 23*, 282–286.

143. Bonnemain, B. (2008) Nanoparticles: the industrial viewpoint. Applications in diagnostic imaging. *Ann. Pharm. Fr. 66*, 263–267.

144. Tang, T. Y., Howarth, S. P. S., Miller, S. R., Graves, M. J., U-King-Im, J. M., Li, Z. Y., Walsh, S. R., Patterson, A. J., Kirkpatrick, P. J., Warburton, E. A., Varty, K., Gaunt, M. E., and Gillard, J. H. (2008) Correlation of carotid atheromatous plaque inflammation using USPIO-enhanced MR imaging with degree of luminal Stenosis. *Stroke 39*, 2144–2147.

145. Jiang, T., Zhang, C., Zheng, X., Xu, X., Xie, X., Liu, H., and Liu, S. (2009) Noninvasively characterizing the different alphavbeta3 expression patterns in lung cancers with RGD-USPIO using a clinical 3.0T MR scanner. *Int. J. Nanomed. 4*, 241–249.

DOI: 10.1021/cn100100e | *ACS Chem. Neurosci.* (2011), *2*, 118–140

146. Das, M., Mishra, D., Dhak, P., Gupta, S., Maiti, T. K., Basak, A., and Pramanik, P. (2009) Biofunctionalized, phosphonate-grafted, ultrasmall iron oxide nanoparticles for combined targeted cancer therapy and multimodal imaging. *Small 5*, 2883–2893.

147. Kiessling, I., Bzyl, J., and Kiessling, F. (2010) Molecular ultrasound imaging and its potential for paediatric radiology, *Pediatr. Radiol.* In press.

148. Meier, R., Henning, T. D., Boddington, S., Tavri, S., Arora, S., Piontek, G., Rudelius, M., Corot, C., and Daldrup-Link, H. E. (2010) Breast cancers: MR imaging of folate-receptor expression with the folate-specific nanoparticle P1133. *Radiology 255*, 527–535.

149. Sudimack, J., and Lee, R. J. (2000) Drug Targeting via the Folate Receptor. *Adv. Drug Delivery Rev. 41*, 147–162.

150. Choi, H., Choi, S. R., Zhou, R., Kung, H. F., and Chen, I. W. (2004) Iron oxide nanoparticles as magnetic resonance contrast agent for tumor imaging via folate receptor-targeted delivery. *Acad. Radiol. 11*, 996–1004.

151. Hogemann, D., Josephson, L., Weissleder, R., and Basilion, J. P. (2000) Improvement of MRI probes to allow efficient detection of gene expression. *Bioconjugate Chem. 11*, 941–946.

152. Hogemann-Savellano, D., Bost, E., Blondet, C., Sato, F., Abe, T., Josephson, L., Weissleder, R., Gaudet, J., Sgroi, D., Peters, P. J., and Basilion, J. P. (2003) The Transferrin Receptor: A Potential Molecular Imaging Marker for Human Cancer. *Neoplasia 5*, 495–506.

153. Kresse, M., Wagner, S., Pfefferer, D., Lawaczeck, R., Elste, V., and Semmler, W. (1998) Targeting of ultrasmall superparamagnetic iron oxide (USPIO) particles to tumor cells in vivo by using transferrin receptor pathways. *Magn. Reson. Med. 40*, 236–242.

154. Radermacher, K. A., Beghein, N., Boutry, S., Laurent, S., Vander Elst, L., Muller, R. N., Jordan, B. F., and Gallez, B. (2009) In vivo detection of inflammation using pegylated iron oxide particles targeted at E-selectin: a multimodal approach using MR imaging and EPR spectroscopy. *Invest. Radiol. 44*, 398–404.

155. Boutry, S., Laurent, S., Elst, L. V., and Muller, R. N. (2006) Specific E-selectin targeting with a superparamagnetic MRI contrast agent. *Contrast Media Mol. Imaging 1*, 15–22.

156. Sigovan, M., Boussel, L., Sulaiman, A., Sappey-Marinier, D., Alsaid, H., Desbleds-Mansard, C., Ibarrola, D., Gamondès, D., Corot, C., Lancelot, E., Raynaud, J. S., Vives, V., Laclédère, C., Violas, X., Douek, P. C., and Canet-Soulas, E. (2009) Rapid-clearance iron nanoparticles for inflammation imaging of atherosclerotic plaque: initial experience in animal model. *Radiology 252*, 401–409.

157. Stoll, G., and Bendszus, M. (2010) New approaches to neuroimaging of central nervous system inflammation. *Curr. Opin. Neurol. 23*, 282–286.

158. Stoll, G., and Bendszus, M. (2009) Imaging of inflammation in the peripheral and central nervous system by magnetic resonance imaging. *Neuroscience 158*, 1151–1160.

159. Nighoghossian, N., Wiart, M., and Berthezene, Y. (2008) Novel applications of magnetic resonance imaging to image tissue inflammation after stroke. *J. Neuroimaging 18*, 349–352.

160. Nighoghossian, N., Wiart, M., Cakmak, S., Berthezène, Y., Derex, L., Cho, T. H., Nemoz, C., Chapuis, F., Tisserand, G. L., Pialat, J. B., Trouillas, P., Froment, J. C., and Hermier, M. (2007) Inflammatory response after ischemic stroke: a USPIO-enhanced MRI study in patients. *Stroke 38*, 303–307.

161. Saleh, A., Schroeter, M., Ringelstein, A., Hartung, H. P., Siebler, M., Mödder, U., and Jander, S. (2007) Iron oxide particle-enhanced MRI suggests variability of brain inflammation at early stages after ischemic stroke. *Stroke 38*, 2733–2737.

162. Jander, S., Schroeter, M., and Saleh, A. (2007) Imaging inflammation in acute brain ischemia. *Stroke 38*, 642–645.

163. Cengelli, F., Maysinger, D., Tschudi-Monnet, F., Montet, X., Corot, C., Petri-Fink, A., Hofmann, H., and Juillerat-Jeanneret, L. (2006) Interaction of functionalized superparamagnetic iron oxide nanoparticles with brain structures. *J. Pharmacol. Exp. Ther. 318*, 108–116.

164. Bierry, G., Jehl, F., Neuville, A., Lefevre, S., Robert, P., Kremer, S., and Dietemann, J. L. (2010) MRI of macrophages in infectious knee synovitis. *AJR, Am. J. Roentgenol. 194*, W521–W526.

165. Bierry, G., Jehl, F., Boehm, N., Robert, P., Dietemann, J. L., and Kremer, S. (2009) Macrophage imaging by USPIO-enhanced MR for the differentiation of infectious osteomyelitis and aseptic vertebral inflammation. *Eur. Radiol. 19*, 1604–1611.

166. Truijers, M., Fütterer, J. J., Takahashi, S., Heesakkers, R. A., Blankensteijn, J. D., and Barentsz, J. O. (2009) In vivo imaging of the aneurysm wall with MRI and a macrophage-specific contrast agent. *AJR, Am. J. Roentgenol. 193*, W437–W441.

167. Saito, T., Abe, T., Tsuchiya, T., Satoh, Y., Kenjo, A., Kimura, T., and Gotoh, M. (2008) Sequential magnetic resonance imaging for evaluation of Kupffer cell function. *Hepatogastroenterology 55*, 596–599.

168. Hyafil, F., Laissy, J. P., Mazighi, M., Tchétché, D., Louedec, L., Adle-Biassette, H., Chillon, S., Henin, D., Jacob, M. P., Letourneur, D., and Feldman, L. J. (2006) Ferumoxtran-10-enhanced MRI of the hypercholesterolemic rabbit aorta: Relationship between signal loss and macrophage infiltration. *Arterioscler., Thromb., Vasc. Biol. 26*, 176–181.

169. Yancy, A. D., Olzinski, A. R., Hu, T. C. C., Lenhard, S. C., Aravindhan, K., Gruver, S. M., Jacobs, P. M., Willette, R. N., and Jucker, B. M. (2005) Differential uptake of ferumoxtran-10 and ferumoxytol, ultrasmall superparamagnetic iron oxide contrast agents in rabbit: Critical determinants of atherosclerotic plaque labeling. *J. Magn. Reson. Imaging 21*, 432–442.

170. Ruehm, S. G., Corot, C., Vogt, P., Kolb, S., and Debatin, J. F. (2001) Magnetic resonance imaging of atherosclerotic plaque with ultrasmall superparamagnetic particles of iron oxide in hyperlipidemic rabbits. *Circulation 103*, 415–422.

171. Van Kasteren, S. I., Campbell, S. J., Serres, S., Anthony, D. C., Sibson, N. R., and Davis, B. G. (2009) Glyconanoparticles

DOI: 10.1021/cn100100e | *ACS Chem. Neurosci.* (2011), *2*, 118–140

allow pre-symptomatic in vivo imaging of brain disease. *Proc. Natl. Acad. Sci. U.S.A. 106*, 18–23.

172. Garca, I., Marradi, M., and Penadés, S. (2010) Glyconanoparticles: Multifunctional nanomaterials for biomedical applications. *Nanomedicine 5*, 777–792.

173. Lepenies, B., and Seeberger, P. H. (2010) The promise of glycomics, glycan arrays and carbohydrate-based vaccines. *Immunopharmacol. Immunotoxicol. 32*, 196–207.

174. Ei-Boubbou, K., Zhu, D. C., Vasileiou, C., Borhan, B., Prospen, D., Wei, L. I., and Huang, X. (2010) Magnetic glyco-nanoparticles: A tool to detect, differentiate, and unlock the glyco-codes of cancer via magnetic resonance imaging. *J. Am. Chem. Soc. 132*, 4490–4499.

175. Geraldes, C. F., Djanashvili, K., and Peters, J. A. (2010) Glycoconjugate probes and targets for molecular imaging using magnetic resonance. *Future Med. Chem. 2*, 409–425.

176. McAteer, M. A., Akhtar, A. M., von zur Muhlen, C., and Choudhury, R. P. (2010) An approach to molecular imaging of atherosclerosis, thrombosis, and vascular inflammation using microparticles of iron oxide. *Atherosclerosis 209*, 18–27.

177. Jin, A. Y., Tuor, U. I., Rushforth, D., Filfil, R., Kaur, J., Ni, F., Tomanek, B., and Barber, P. A. (2009) Magnetic resonance molecular imaging of post-stroke neuroinflammation with a P-selectin targeted iron oxide nanoparticle. *Contrast Media Mol. Imaging 4*, 305–311.

178. Berger, C., Hiestand, P., Kindler-Baumann, D., Rudin, M., and Rausch, M. (2006) Analysis of lesion development during acute inflammation and remission in a rat model of experimental autoimmune encephalomyelitis by visualization of macrophage infiltration, demyelination and blood-brain barrier damage. *NMR Biomed. 19*, 101–107.

179. Cunningham, C. H., Arai, T., Yang, P. C., McConnell, M. V., Pauly, J. M., and Conolly, S. M. (2005) Positive contrast magnetic resonance imaging of cells labeled with magnetic nanoparticles. *Magn. Reson. Med. 53*, 999–1005.

180. Anderson, S. A., Rader, R. K., Westlin, W. F., Null, C., Jackson, D., Lanza, C. M., Wickline, S. A., and Kotyk, J. J. (2000) Magnetic resonance contrast enhancement of neovasculature with alpha(v)beta(3)-targeted nanoparticles. *Magn. Reson. Med. 44*, 433–439.

181. Polyak, B., and Friedman, G. (2009) Magnetic targeting for site-specific drug delivery: applications and clinical potential. *Expert Opin. Drug Delivery 6*, 53–70.

182. Amiri, H., Mahmoudi, M., and Lascialfari, A. (2011) Superparamagnetic colloidal nanocrystal clusters coated with polyethylene glycol fumarate: a possible novel theranostic agent, *Nanoscale*. DOI: 10.1039/c0nr00603c.

183. Jalilian, A. R., Panahifar, A., Mahmoudi, M., Akhlaghi, M., and Simchi, A. (2009) Preparation and biological evaluation of [67Ga]-labeled- superparamagnetic nanoparticles in normal rats. *Radiochim. Acta 97*, 51–56.

184. Bartolozzi, C., Lencioni, R., Donati, F., and Cioni, D. (1999) Abdominal MR: Liver and pancreas. *Eur. Radiol. 9*, 1496–1512.

185. Meng, J., Fan, J., Galiana, G., Branca, R. T., Clasen, P. L., Ma, S., Zhou, J., Leuschner, C., Kumar, C. S. S. R., Hormes, J., Otiti, T., Beye, A. C., Harmer, M. P., Kiely, C. J., Warren, W., Haataja, M. P., and Soboyejo, W. O. (2009) LHRH-functionalized superparamagnetic iron oxide nanoparticles for breast cancer targeting and contrast enhancement in MRI. *Mater. Sci. Eng., C 29*, 1467–1479.

186. Shubayev, V. I., Pisanic, Ii, T. R., and Jin, S. (2009) Magnetic nanoparticles for theragnostics. *Adv. Drug Delivery Rev. 61*, 467–477.

187. Matthews, P. M. (2009) Brain Imaging of Multiple Sclerosis: the Next 10 Years. *Neuroimaging Clin. North Am. 19*, 101–112.

188. Hauser, S. L., and Oksenberg, J. R. (2006) The Neurobiology of Multiple Sclerosis: Genes, Inflammation, and Neurodegeneration. *Neuron 52*, 61–76.

189. Baranzini, S. E., Galwey, N. W., Wang, J., Khankhanian, P., Lindberg, R., Pelletier, D., Wu, W., Uitdehaag, B. M. J., Kappos, L., Polman, C. H., Matthews, P. M., Hauser, S. L., Gibson, R. A., Oksenberg, J. R., and Barnes, M. R. (2009) Pathway and network-based analysis of genome-wide association studies in multiple sclerosis. *Hum. Mol. Genet. 18*, 2078–2090.

190. Baranzini, S. E., Srinivasan, R., Khankhanian, P., Okuda, D. T., Nelson, S. J., Matthews, P. M., Hauser, S. L., Oksenberg, J. R., and Pelletier, D. (2010) Genetic variation influences glutamate concentrations in brains of patients with multiple sclerosis. *Brain 133*, 2603–2611.

191. Mikita, J., Dubourdieu-Cassagno, N., Deloire, M. S., Vekris, A., Biran, M., Raffard, G., Brochet, B., Canron, M. H., Franconi, J. M., Boiziau, C., Petry, K. G. (2010) Altered M1/M2 activation patterns of monocytes in severe relapsing experimental rat model of Multiple Sclerosis. Amelioration of clinical status by M2 activated monocyte administration, *Mult. Scler.*, PMID: 20813772.

192. Dousset, V., Brochet, B., Deloire, M. S. A., Lagoarde, L., Barroso, B., Caille, J. M., and Petry, K. G. (2006) MR imaging of relapsing multiple sclerosis patients using ultra-small-particle iron oxide and compared with gadolinium. *American Journal of Neuroradiology 27*, 1000–1005.

193. Matthews, P. M., and Comley, R. (2009) Advances in the molecular imaging of multiple sclerosis. *Expert Review of Clinical Immunology 5*, 765–777.

194. Conturo, T. E., Akbudak, E., Kotys, M. S., Chen, M. L., Chun, S. J., Hsu, R. M., Sweeney, C. C., and Markham, J. (2005) Arterial input functions for dynamic susceptibility contrast MRI: Requirements and signal options. *J. Magn. Reson. Imaging 22*, 697–703.

195. Jalilian, A. R., Hosseini-Salekdeh, S. L., Mahmoudi, M., Yousefnia, H., Majdabadi, A., and Pouladian, M. (2010) Preparation and biological evaluation of radiolabeled-folate embedded superparamagnetic nanoparticles in wild-type rats, *J. Radioanal. Nucl. Chem.* In press.

196. Vellinga, M. M., Oude Engberink, R. D., Seewann, A., Pouwels, P. J. W., Wattjes, M. P., Van Der Pol, S. M. A., Pering, C., Polman, C. H., De Vries, H. E., Geurts, J. J. G., and Barkhof, F. (2008) Pluriformity of inflammation in multiple sclerosis shown by ultra-small iron oxide particle enhancement. *Brain 131*, 800–807.

197. Harris, V. K., and Sadiq, S. A. (2009) Disease biomarkers in multiple sclerosis: potential for use in therapeutic decision making. *Mol. Diagn. Ther. 13*, 225–244.

198. Cheng, M. M., Cuda, G., and Bunimovich, Y. L. (2006) Nanotechnologies for biomolecular detection and medical diagnostics. *Curr. Opin. Chem. Biol. 10*, 11–19.

199. Lin, L. N., Liu, Q., Song, L., Liu, F. F., and Sha, J. X. (2010) Recent advances in nanotechnology based drug delivery to the brain, *Cytotechnology*, in press.

200. Calvo, P., Gouritin, B., Villarroya, H., Eclancher, F., Giannavola, C., Klein, C., Andreux, J. P., and Couvreur, P. (2002) Quantification and localization of PEGylated polycyanoacrylate nanoparticles in brain and spinal cord during experimental allergic encephalomyelitis in the rat. *Eur. J. Neurosci. 15*, 1317–1326.

201. Neuberger, T., Schpf, B., Hofmann, H., Hofmann, M., and von Rechenberg, B. (2005) Superparamagnetic nanoparticles for biomedical applications: Possibilities and limitations of a new drug delivery system. *J. Magn. Magn. Mater. 293*, 483–496.

202. Abu-Lail, N. I., Kaholek, M., LaMattina, B., Clark, R. L., and Zauscher, S. (2006) Micro-cantilevers with end-grafted stimulus-responsive polymer brushes for actuation and sensing. *Sens. Actuators, B 114*, 371–378.

203. Tanaka, T., and Fillmore, D. J. (1979) Kinetics of swelling of gels. *J. Chem. Phys. 70*, 1214–1218.

204. Santer, S., Kopyshev, A., Donges, J., Yang, H. K., and Ruhe, J. (2006) Dynamically reconfigurable polymer films: Impact on nanomotion. *Adv. Mater. 18*, 2359–2362.

205. Motornov, M., Sheparovych, R., Tokarev, I., Roiter, Y., and Minko, S. (2007) Nonwettable thin films from hybrid polymer brushes can be hydrophilic. *Langmuir 23*, 13–19.

206. Crowe-Willoughby, J. A., and Genzer, J. (2009) Formation and properties of responsive siloxane-based polymeric surfaces with tunable surface reconstruction kinetics. *Adv. Funct. Mater. 19*, 460–469.

207. Stuart, M. A. C., Huck, W. T. S., Genzer, J., Muller, M., Ober, C., Stamm, M., Sukhorukov, G. B., Szleifer, I., Tsukruk, V. V., Urban, M., Winnik, F., Zauscher, S., Luzinov, I., and Minko, S. (2010) Emerging applications of stimuli-responsive polymer materials. *Nat. Mater. 9*, 101–113.

208. Paolicelli, D., Direnzo, V., and Trojano, M. (2009) Review of interferon beta-1b in the treatment of early and relapsing multiple sclerosis. *Biologics 3*, 369–376.

209. Burtea, C., Laurent, S., Port, M., Lancelot, E., Ballet, S., Rousseaux, O., Toubeau, G., Vander Elst, L., Corot, C., and Muller, R. N. (2009) Molecular MRI of VCAM-1 expression in inflammatory lesions by using a peptide-vectorized paramagnetic imaging probe. *J. Med. Chem. 52*, 4725–4742.

DOI: 10.1021/cn100100e | *ACS Chem. Neurosci.* (2011), *2*, 118–140